AAEC/TM390

AUSTRALIAN ATOMIC ENERGY COMMISSION

RESEARCH ESTABLISHMENT
LUCAS HEIGHTS

FEASIBILITY DESIGN OF PRESTRESSED CONCRETE PRESSURE VESSELS FOR HIGH PRESSURE GAS COOLED REACTORS

by

A. SPENCER

May 1967

AUSTRALIAN ATOMIC ENERGY COMMISSION

RESEARCH ESTABLISHMENT

LUCAS HEIGHTS

FEASIBILITY DESIGN OF PRESTRESSED CONCRETE PRESSURE VESSELS FOR HIGH PRESSURE GAS COOLED REACTORS

by

A. SPENCER

ABSTRACT

The design philosophy of prestressed concrete pressure vessels is examined with particular reference to the design for a 200MWe H.T.G.C. Reactor. Equations for preliminary design and costing of such vessels are derived, and their use for optimization is demonstrated. Considerable design investigation in support of the methods used is presented as appendices to the report.

CONTENTS

Continued...

CONTENTS (Continued)

Continued...

CONTENTS (Continued)

1. INTRODUCTION

The A.A.E.C.'s reference design study of a 200 MWe pebble bed reactor, based on moderation by beryllia (Ebeling and Hayes 1967) required the containment of high temperature carbon dioxide at 1000 p.s.i.g. The minimum inside diameter of the containing vessel would be 28 ft. In steel, such a vessel would have to be 10 inches thick if cylindrical or 5 inches thick if spherical. For the reference design, prestressed concrete was chosen for economy and to avoid the welding of such heavy steel plates. Further, it was considered that a prestressed concrete pressure vessel (P.C.P.V.) could be built by Australian contractors, and if remote sites were to be used the penalty in transport or construction costs would be less than for steel vessels.

The design of P.C.P.V.s was investigated with two aims:

(1) To establish their technical feasibility by considering and determining all features which might make the design impractical.

(2) To determine which design would give the greatest economy in the overall cost of the plant, that is, to optimize cost, to achieve economic feasibility.

A tall cylindrical, rather than spherical, vessel was chosen not only because the proposed reactor plant could advantageously be arranged in a cylinder, but because spherical vessels have several associated problems, that is, tendon arrangements are complex, especially because of anchorage requirements, and forming and pouring is difficult. Modified spherical designs such as Wylfa (Taylor and Williams 1964) and EDF3 (Lamiral et al. 1964) seem to show little gain over cylindrical designs, and make analysis more difficult. The fact that the design for EDF4, which followed EDF3 was a tall cylindrical vessel, seemed to favour the chosen arrangement. (Refer also to Houghton-Brown, Harris et al. 1964).

The chosen tendon arrangement and the general arrangement of the vessel are shown in Figure 1. The helical tendon arrangement used for the Oldbury vessel (Houghton-Brown, Hay, et al. 1964) was considered but, as shown in Appendix 8, it is only suitable for squat vessels.

The flat slabs for the ends were chosen to simplify construction. They introduce discontinuity stresses where they join the cylinder wall, and they may not fail progressively. But the design proposed for them meets these objections; alternatives, such as tension or compression domes, are difficult to construct and also such designs do not give complete theoretical satisfaction.

A set of equations was derived for determining the dimensions of the required P.C.P.V. given inside size, and pressure. A cost derivation based on the generalised dimensions obtained is given in Appendix 11. From these relationships, using a computer programme (Hope A.A.E.C. unpublished), some curves showing design and cost trends were obtained. Several interesting trends became apparent.

The analysis is essentially simple. It might not be used for the final design of a vessel, but it does give realistic dimensions which are quite adequate for feasibility studies. (Elaborate elastic analysis of concrete stresses might not be used for a final design either because the marked inelastic properties of concrete can produce quite different behaviour.) Similarly, the costing is not sufficiently detailed for tendering, but it is sufficiently reliable for optimization.

The methods were developed for an investigation of a high temperature gas cooled reactor, but they are equally applicable to other types, for example, a gas cooled, heavy water moderated reactor, or even a water cooled reactor, if lining and insulation problems can be overcome.

2. SAFETY OF PRESTRESSED CONCRETE PRESSURE VESSELS

Prestressed concrete pressure vessels are inherently safer than steel vessels, that is, complete rupture would be incredible in a satisfactorily designed and operated vessel. This is because the integrity of the vessel depends primarily on the tendons, and they can be relied on absolutely for the following reasons:

(1) They are stressed only in pure tension, with neither bending nor significant secondary stresses.

(2) The maximum load to which they will be subject is applied when they are initially tensioned. This constitutes a proof load, guaranteeing reliability.

(3) After tensioning, even full depressurization cycles will vary tendon load by less than 7 per cent so tendon stress may be regarded as constant.

(4) In normal designs, tendons are adequately shielded from irradiation and all but very slow temperature variations. Designs providing for the inhibition of corrosion are possible for practical tendon systems.

(5) Factors already mentioned confer a high probability that tendons will not fail in service, but some of the benefit of this is reduced by operating at a stress of about 60 per cent of ultimate stress. The really significant factor is the very large number of tendons. The

failure of one, or even several tendons, throws only a slight increase of load on to the remaining ones.

(6) If the tendons are left ungrouted, they can be removed for replacement if they fail, or removed on some routine basis to examine them for signs of corrosion or other damage. But the French, for example, grout the tendons, believing that the assurance against corrosion so obtained is sufficient to ensure reliable service.

But careful design is necessary to ensure that the integrity of the vessel is guaranteed by the tendons. The disposition of tendons to hold the concrete together after it has cracked, without the risk of an unstable collapse, is quite critical. Waters and Barrett (1963) describe the philosophy of 'progressive failure', which requires that there be no sudden complete failure without warning. Ultimate failure must only occur after a series of distortions, cracks or other detectable effects. Provision of sufficient safety valves guarantees that failure as a result of generation of excess pressure will not occur, but rather from some material deterioration. The progressive failure postulated is therefore unlikely to happen other than slowly, allowing corrective action to be taken.

Consequently, the 'maximum credible accident' for a properly designed P.C.P.V. can be taken to be the blowing out of a penetration. By limiting the size of penetrations, secondary containment requirements can be kept small.

3. DESIGN

3.1 Limiting Pressures

Given the working pressure p_w, three limiting conditions of pressure are defined:

(a) Ultimate pressure, p_u, at which the concrete of the cylinder wall has fully cracked radially and the tendons have reached their minimum breaking strength. This condition determines the number of tendons required. It is defined by a load factor β, applied to p_w.

Reported tests to destruction of P.C.P.V. models show that provided there is sufficient margin to p_u above the concrete cracking pressure p_{cc}, the liner fails, and the gas vents, before any tendons break. Thus p_u is never attained. For a particular design it would seem desirable to demonstrate this property, although as mentioned above, failure in practice will not be due solely to pressure rise. Noting the values of load factor reported for designs based on such model

tests, and Waters and Barrett's (1963) recommendations, a value for β of 2.75 was chosen.

Having chosen a load factor β it must be shown that venting of gas through a crack in the wall does not cause tendon failure. This condition is most severe for horizontal cracks, and the necessary value of β will depend on the ratio α of the outside diameter d_o, to the inside diameter d_i. On the simplified, but conservative, assumption that the pressure at the entry to the crack falls to half the vessel pressure (which can be as high as the safety valve relief pressure) and drops off linearly to zero at the outside, $\beta = 2.6$ is sufficient for values of α up to 2. (This may be insufficient for water/steam). Note also that a significant leak which developed in the vessel liner for any reason could be expected to drive a horizontal crack right through the concrete. This condition requires experimental elaboration, but depressurization, with no tendon failure, could be expected. This is discussed in Appendix 10.

(b) No internal pressure, when the concrete must withstand the full initial prestress.

(c) Test pressure, applied to ensure acceptable strain behaviour to a pressure in excess of the safety valve relief pressure (and also to ensure leak tightness of the liner). Test pressure was taken to be 1.15 × S.V. relief pressure, or 1.265 p_w. A margin of 5 per cent was allowed above the test pressure, to the value used for design (referred to as the 'test design pressure'). Only at this value would the design tensile stress be reached in the concrete, and then only after full tendon relaxation had occurred. At the actual test pressure, a tensile stress less than 100 p.s.i. could be expected in the concrete behind the liner.

Some engineers hold that no primary tensile stress should be permitted in the concrete under any conditions. Thus in defence of the criteria adopted, it is pointed out that there will be shrinkage cracks in the concrete anyway, and that the presence of well distributed (by reinforcement) fine cracks does not necessarily impair the performance of the vessel.

The foregoing pressure conditions are sufficient to determine vessel dimensions and tendon arrangements, but when considering safety, and ultimate failure conditions, a further pressure may be defined. This is the pressure at which, due to primary stress alone, the concrete will have failed in tension (that is, concrete tensile

stress 600 p.s.i). Above this pressure, all load must be borne by the tendons and by reinforcement. For safety there should be an adequate margin between this pressure and the ultimate pressure to ensure depressurization before tendon failure. It can be shown that the concrete cracking pressure = 1.15 p_{td} for all values of working pressure.

Pressure relations can now be summarised:

Safety valve relief pressure	=	1.10 p_w
Test pressure	=	1.265 p_w
Test design pressure p_{td}	=	1.33 p_w
Concrete cracking pressure	=	1.53 p_w
Ultimate pressure p_u	=	2.75 p_w

3.2 Allowable Stresses

Under the limiting pressure conditions defined, the material strengths are conditioned by temperature, humidity, radiation, etc., and they must cover the effects of strain dependent or secondary stresses. This has been done by taking primary stress at working pressure as one third of failure stress under the conditions found.

For concrete, a cylinder strength at 28 days of 6000 p.s.i. at 70°C is assumed. A tensile strength one tenth of this is assumed, that is, 600 p.s.i., so that design tensile strength, f_t is taken as 200 p.s.i. This may be compared with the often used value 3 $\sqrt{\text{cylinder strength}}$, or 230 p.s.i.

The work of Bellamy (1961) at the University of Sydney in 1959 has been used to derive increased values of safe compressive stress for critical areas. At these areas, compressive stress is applied in at least two of the three possible axes, and compressive failure is inhibited up to much higher values than for uniaxial compression. These effects are examined briefly in Appendix 1. 2500 p.s.i. is taken for f_c on the inside face of the cylinder wall, and at the centre of the inner face of the end slabs. These are the most restrictive areas for compressive stress, and are limiting on the design. For uniaxial compression, f_c is, of course, 2000 p.s.i.

For the P.C.P.V. of the reference design (Ebeling and Hayes 1967) a simple calculation showed that the maximum thermal stress difference due to radiation heating in the concrete near the inner face of the cylinder wall would be less than 1000 p.s.i. Of this, 500 p.s.i. might appear as tension on the inner face,

but it would be quite nullified by the compressive stress resulting from only a small overall temperature drop to the outside of the wall. The other 500 p.s.i. of thermal stress difference would be additive to the compressive stress due to overall temperature drop through the wall. For each design this must be checked, and in a cold climate it might be necessary to restrict the rate at which building ventilation removes heat from the outside of the vessel.

A further reason for controlling the temperature of the outer face of the wall, is to restrict thermal tensile strain there. But fine cracking on the outer face is not likely to be significant, so the provision of reinforcement for crack distribution may be all that is required.

It is probably desirable to limit compressive thermal stress near the inside cylinder wall to the same value as the primary stress. This leaves a further margin to failure of the same order to allow for discontinuity stresses. It might be thought that insufficient stress margin remains to failure, but it seems to be generally accepted that creep in concrete can readily deal with strain dependent stresses, provided only that their rate of change is sufficiently restricted.

The tendons are assumed to be 12/0.6 in. with a minimum breaking load, allowing 95 per cent anchor efficiency, of 740,000 lb. The economic advantage of using larger tendons is likely to be small, so it is better to choose a stock tendon similar to those already in use for conventional structures. The jacking load is calculated to result in a working load 60 per cent of ultimate, but as shown later, variation from 60 per cent has little effect.

3.3 Design of End Slabs

When discussing the safety of P.C.P.V.s, and the choice of load factor, cracking was considered as limited to the cylinder wall. This is because the ultimate failure of prestressed slabs may not be 'progressive', but sudden (Campbell-Allen and Low 1967; Warner 1964). To ensure 'progressive failure', the end slabs are designed to withstand ultimate pressure, with design stress values.

Figure 1 shows the arrangement of end slabs chosen. Three systems of straight tendons, oriented horizontally at 60° to each other, are used. This arrangement best suited the hexagonal arrangement of penetrations for control rods and fuel ball feeders. It also gave a hexagonal slab which matched well with the six rib arrangement for cylinder tendons. But two, or four, systems of tendons could be used, and perhaps even more. The analysis is basically the same.

The limiting design conditions for the end slabs are given by Equations 4 and 5 of Appendix 2:

$$\sigma_{ps(u)} - \sigma_{r(u)\ (r=o)} = f_t \qquad .....3.1$$

$$\sigma_{ps(u)} + \sigma_{r(u)\ (r=o)} = f_c \qquad .....3.2$$

Substituting for $\sigma_{ps(u)}$ from Equation 3 of Appendix 2, and for $\sigma_{r(u)\ (r=o)}$ from Equation 3 of Appendix 3, the following simple expressions for slab prestress and thickness, are obtained:

$$T_u/S_h S_v = 0.575\ (f_c + f_t) \qquad .....3.3$$

$$t = r_o \sqrt{\frac{1.275\ \beta\ p_w}{f_c - f_t}} \qquad .....3.4$$

A final condition, to ensure that the slab does not fail in shear at the edges, is derived in Appendix 4. The maximum principal tensile stress under ultimate pressure conditions is held to the design value of tensile stress in the concrete. The results of Campbell-Allen and Low (1967) show that this is a conservative, if not completely accurate, criterion. The limiting value of slab thickness is given by Equation 6 of Appendix 4:

$$t = 0.75\ p_u\ r_o \left[\left(\frac{0.435\ T_u}{S_h\ S_v} + \frac{P_u}{4} - f_t \right)^2 - \left(\frac{0.435\ T_u}{S_h\ S_v} - \frac{p_u}{4} \right)^2 \right]^{-\frac{1}{2}} \qquad .....3.5$$

The final thickness of the slab is attained by adding say 3 feet of concrete on the inside to shield the cables. Because each system of cables must completely cover the pressure loaded area of the slab, the sides of the hexagon must be not less than d_i in length, and the distance across flats then becomes $1.73\ d_i$. The following relations follow from these considerations:

$$t_s = t + 3 \text{ feet} \qquad .....3.6$$

$$n_e = 3\ \frac{d_i}{S_h} \cdot \frac{t}{S_v} \qquad .....3.7$$

$$L_e = 1.75\ d_i \qquad .....3.8$$

If relative values of S_h and S_v are determined from practical considerations the design of the end slabs is fully specified.

3.4 Design of Cylinder Wall

The cylinder is treated as a tube, but because the wall is very thick by comparison with its diameter, thin-tube equations cannot be used. There is evidence to suggest that creep plays a significant role in relieving elastic stress concentrations in concrete. But if fully elastic conditions are assumed, and the Lamé equation applied, a conservative design must result. It can be demonstrated that the limiting concrete primary stresses, either compressive or tensile, will occur on the inside face of the cylinder wall. The value of these circumferential stresses is given by the formula:

$$\sigma_i = \left[2\, p_o d_o^2 - p_i\, (d_o^2 + d_i^2) \right] \Big/ \left[d_o^2 - d_i^2 \right] \quad . \qquad .....3.9$$

In this equation, because pressures are compressive, it is convenient to call compressive stress positive and tensile stress negative. It is simplified if αd_i is substituted for d_o:

$$\sigma_i = \left[2\, p_o \alpha^2 - p_i(\alpha^2 + 1) \right] \Big/ \left[\alpha^2 - 1 \right] \quad . \qquad .....3.10$$

The external pressure p_o represents the inward force of the tendons, considered as acting at the single diameter d_o, and will have its highest value during tensioning; this constitutes one limit on the design. That is, put $p_o = p_{s(ten)}$, $p_i = 0$, and $\sigma_i = f_c$.

$$\text{Then } f_c = 2\, p_{s(ten)}\, \alpha^2/(\alpha^2 - 1) \quad . \qquad .....3.11$$

The external pressure p_o will have a lower value when the test pressure is applied to the vessel, and this constitutes the other limit on the design. That is, put $p_o = p_{s(td)}$, $p_i = p_{td}$ and $\sigma_i = f_t$.

$$\text{Then } f_t = \left[2\, p_{s(td)}\, \alpha^2 - p_{td}\, (\alpha^2 + 1) \right] \Big/ \left[\alpha^2 - 1 \right] \quad . \qquad .....3.12$$

Equivalent equations for the vertical stress in the concrete, if it is assumed to be distributed uniformly between d_i and d_o, are:

$$f_c = 4\, n_v\, T_{v(ten)} \Big/ \pi(\alpha^2 - 1)\, d_i^2 \quad , \qquad .....3.13$$

$$f_t = \left[4\, n_v\, T_{v(td)} - \pi\, p_{td}\, d_i^2 \right] \Big/ \pi \left[\alpha^2 - 1 \right] d_i^2 \quad . \qquad .....3.14$$

These equations are of limited accuracy, but they serve to show that the vertical concrete stresses are not limits on the design.

3.5 Tendon Design for Cylinder Wall

The arrangement of circumferential tendons is shown by Figure 2, together with the dimensions used to define it. It is a flexible arrangement, permitting the use of any wrap angle, and any number of ribs up to eight. The limit at eight is to allow clearance for threading and tensioning. Six were chosen for the reference design because six boilers with six sets of penetrations, fitted well with the hexagon based arrangement of control rods inside the vessel. As will be seen later, six gives good economy.

An alternative arrangement of circumferential tendons, with 20 ribs, and the tendons running between them in the open, was examined because it reduced the clearance dimensions of the vessel and seemed to offer a reduction in cost. However, it was rejected because the large number of tendons required for a high vessel pressure made the design of the ribs doubtful.

Another type of arrangement is to form the outer surface of the cylinder as a hexagon, and anchor the tendons on the corners. This was rejected because not enough volume seemed to be available for the large number of anchors required. Further, it offered no gain in clearance dimensions over the ribbed arrangement.

3.5.1 Tendon friction and relaxation

If the working load in the circumferential tendons, due to prestress alone, is not to exceed 60 per cent of the ultimate, the limiting values for design use (See Appendix 5) are:

$$T_{\theta_o(ten)} = 0.62\, T_u \qquad .....3.15$$

$$T_{\theta_o(td)} = 0.58\, T_u \quad . \qquad .....3.16$$

T_{θ_o} is the maximum tension in the anchored tendon, assumed to occur at the edge of the rib in which it is anchored (See Figure 2). $T_{\theta_o\,(ten)}$ is the maximum effective value likely to occur during the tensioning period of several months, and $T_{\theta_o(td)}$ is the fully relaxed value, which may have been reached when the test pressure is applied. For the vertical tendons in the cylinder wall, the same considerations apply, and similar equations are obtained:

$$T_{v(ten)} = 0.62\, T_u \qquad .....3.17$$

$$T_{v(td)} = 0.58\, T_u \qquad .....3.18$$

3 5.2 Tendon pressure under ribs

In Appendix 6, it is shown that the crossed straight tendon ends in the anchor ribs, can be regarded as a single continuous curved tendon. The tension assumed to be in it can be T_{θ_o} (or 0.995 T_{θ_o} if this accuracy is justified).

3.5.3 Equivalent tendon position

For practical arrangements, as shown in Figure 2, the tendons are distributed radially over a band of width b. For design equations giving values of circumferential stress in the concrete at d_i, it is convenient to assume the tendons to be concentrated at an equivalent band diameter d_o.

If each tendon contributes the same stress to the concrete as it would if it were acting alone, it can be shown that:

$d_o \approx$ mean band diameter.

The accuracy of this is seen in Figure 3, for compressive and tensile stress in the concrete, as given respectively by Equations 3.11 and 3.12. Since band widths are unlikely to be greater than a third of the wall thickness, the error introduced by this assumption will be less than 0.5 per cent.

The reason for making this assumption is that the calculation of the true effective diameter, as performed in deriving the curves of Figure 3, involves a separate stress calculation for each tendon, and subsequent summation, which is a very cumbersome process.

3.5.4 Tendon tension and concrete stress

For the type of arrangement shown by Figure 2, values of maximum and minimum effective average tension for circumferential tendons, (Appendix 7) can be obtained from the formula:

$$T_{ea} = \frac{T_{\theta_o}}{n_z}\left[e^{-\mu(\phi - \frac{\theta_r}{2})} + e^{-\mu(2I\phi_M - \frac{\theta_r}{2} - \phi)} + e^{-\mu(2I\phi_M - \frac{\theta_r}{2} + \phi)}\right] , \qquad \text{.....3.19}$$

where: I is given all the integer values from 1 to $\frac{n_z}{2}$ (or the nearest smaller integer), and

the last term is omitted if n_z is even, that is, there must always be a total of n_z terms in the brackets.

In Equation 3.19 the angle ϕ_M is given by:

$$\phi_M = \pi/r. \qquad \text{.....3.20}$$

The tensioned tendons exert an inward pressure on the vessel given by:

$$p_s = 2\, n_z\, n_b\, T_{ea}/d_o h \quad . \qquad \text{.....3.21}$$

The values of p_s required for determination of wall thickness are given by Equation 3.21, using the following values in Equation 3.19.

For $T_{\theta_o} = T_{\theta_o(ten)}$ and $\phi = \theta_r/2$, $p_s = p_{s(ten)}$ 3.22

For $T_{\theta_o} = T_{\theta_o(td)}$ and $\phi = \phi_M = \pi/r$, $p_s = p_{s(td)}$ 3.23

For the vertical tendons, run in smooth straight tubes, friction may be neglected, so the values of $T_{v(ten)}$ and $T_{v(td)}$ given in Section 3.5.1 may be used directly in Equations 3.13 and 3.14 to determine concrete stress.

3.5.5 The number of tendons required

For all but very high pressures, the number of tendons required is determined by considering ultimate pressure in the vessel, and the cylinder walls fully cracked, but held together by the tendons at their ultimate load. Considering the circumferential and vertical tendons independently, force balances give:

$$2\, n_z\, n_b\, T_u/h = p_u\, d_i \qquad \text{.....3.24}$$

$$n_v\, T_u = \frac{\pi}{4}\, d_i^2\, p_u \quad . \qquad \text{.....3.25}$$

3.5.6 Tendon arrangement

Referring again to Figure 2, the following relations should be noted:

$$\cos\theta_r = (d_o - X)/(d_o + X) \qquad \text{.....3.26}$$

$$D_o = d_o + X \qquad \text{.....3.27}$$

$$A = D_o \sin\frac{\theta_r}{2} \qquad \text{.....3.28}$$

$$a = (D_o - 2X)\sin\frac{\theta_r}{2} \qquad \text{.....3.29}$$

$$L_c = \frac{d_o}{2}\,\theta_w + (d_o - b)\tan\theta_r \qquad \text{.....3.30}$$

$$L_v = H + 2t_s \qquad \text{.....3.31}$$

$$r(\theta_w + \theta_r) = 2\pi n_z \quad . \qquad \text{.....3.32}$$

Choosing 11 inches as the minimum centre to centre spacing of tendon tubes, to permit proper concrete placing, and putting the edge clearance, C = 8 inches.

$$h = 11\, n_z \text{ inches} \quad \text{.....3.33}$$

$$b = 11\,(n_b - 1) \text{ inches} \quad \text{.....3.34}$$

$$X = (n_b - 1)\,11 + 16 \text{ inches} \quad \text{.....3.35}$$

Noting that the number of tendon anchors will be twice the number of tendons, it is evident that the geometry of tendons and concrete has been fully defined.

3.6 Connection of Wall and Slabs

Connection of wall and slabs is a weak point of the simple arrangement chosen. In particular, the deliberate over-design of the end slabs will impose even higher discontinuity stresses, and cracking is first likely to appear radially across the wall just under the slab. This would not be a disadvantage under ultimate conditions, but could limit elastic behaviour.

A means of limiting the formation of a crack across the wall under the slab is to increase the number of vertical tendons above that required by Equation 3.25, to that permitted by Equation 3.13, that is, to put in more tendons than necessary to contain the ultimate pressure, but not enough to over-stress the concrete in compression. This cannot be treated other than as a separate detailed study, supported by model tests, particularly because of the following dependent effects:

1. Increase in tendon cost.
2. Effect on failure mode of the end slabs.
3. Effect on failure mode of the cylinder wall, and margin between cracking pressure and ultimate pressure.
4. Establishment of more biaxial constraint, permitting a higher compressive stress in the concrete, and possible reduction in wall thickness.
5. Balancing of vertical and circumferential stresses in the concrete, permitting reduction of penetration liner thickness.

The addition of tendons would of course increase the tendon cost, but if as a result the wall thickness and penetration liner thickness can be reduced, the total cost may not increase. Thus for simplicity in deriving significant cost trends it seems reasonable to neglect this addition.

The feasibility of the connection of the stiff slabs to the cylinder wall is judged to be not in doubt for the following reasons:

1. There is scope for more than doubling the vertical tendons, so it should be possible to reduce the probability of cracking horizontally at the connection, to that of cracking vertically in the wall.
2. Extra bonded reinforcement can be provided to limit and distribute cracks, as well as to resist shear stress arising from the restraint of the stiff slab on the wall.
3. An ample fillet can be provided on the inside corner to distribute cracks further.
4. Concrete is able to creep off stress concentration.
5. Model tests reported in the literature (particularly Warner 1964) confirm the satisfactory behaviour of similar designs.

It may be noted that vertical bending stresses in the cylinder wall can be calculated if the wall is regarded as a number of parallel beams spanning between the end slabs. We have regarded the cylinder wall as a tube with discontinuity stresses applied at the ends by the restraint of the end slabs. From either point of view, adjustment of the number of vertical tendons should enable the vertical stresses to be held lower than the circumferential stresses, which have been regarded as limiting.

3.7 Other Design Aspects

Aspects already discussed determine the main dimensions of the vessel but there are further aspects quite vital to the operation of the vessel, and of very significant cost, which are now described briefly:

3.7.1 Internal lining

The lining on the inside of the wall of the P.C.P.V. has several functions:

1. To provide an impermeable barrier to the contained fluid to a pressure which is well in excess of the cracking pressure. (For design purposes, aim to just contain the ultimate pressure.)
2. To withstand many cycles of severe strain.
3. To withstand, without buckling, compressive strain up to yield, imposed by prestress and thermal effects.
4. To transmit all the heat it gains from the contained fluid, to the cooling system, without significant heating of the concrete.
5. To act as a self-supporting concrete former.

6. As a requirement of several of the above functions, to maintain ductility, necessitating adequate shielding.

Ductile mild steel, $\frac{3}{4}$ inch thick was chosen. Thicknesses used elsewhere are Oldbury $\frac{1}{2}$ inch, Wylfa $\frac{3}{4}$ inch and in France 1 inch and over.

The liner is stiffened and anchored by continuous 1 inch M.S. ribs 6 inches deep, spaced at 12 inches. These anchor ribs must be capable of resisting a shearing force limited only by the compressive yield stress of the liner. Because ultimate shear stress $\approx \frac{3}{4}$ of yield stress, ribs 1 inch thick are required.

Problems of compressive strain beyond yield, large strain cycling, and buckling, have been well described by Beer (1964). There seems to be no problem with ductile mild steel, provided the anchor spacing is < 100 times liner thickness.

For an ultimate pressure of 2750 p.s.i. a $\frac{3}{4}$ inch liner should bridge a $4\frac{1}{2}$ inch crack without failure. Such a single crack could occur in a vessel of overall height 100 ft, if the full tendon extension to failure appeared at it. But a liner securely anchored to the wall, would be drawn over this distance, and might well tear. Thus, bonded reinforcement must be provided to distribute cracks, and the thickness of liner required for a given failure pressure can only be estimated from model tests.

With the cooling system provided, the liner thickness is adequate for heat transfer. With one circuit out of operation, the highest liner temperature is 20°C above cooling tube temperature. (Refer to Figure 4).

3.7.2 Internal insulation

Insulation is provided to limit heat loss, and to reduce the duty of the liner and cooling system in keeping the concrete cool. For this design, heat loss was restricted to 1 MW using dimpled stainless steel foil of the thicknesses specified in Figure 4. Because this insulation is extremely expensive, optimization of its thickness against heat loss would be justified in a final design. Very significant cost reductions could be made if a cheaper insulation, of proved reliability, could be found. A major problem is penetration of the insulation by the high pressure gas, and resulting insulation destruction in the event of depressurization. With S.S. foil, escape paths can be left.

If a liquid is contained instead of gas, additional compatibility problems arise, not only with the insulation, but also the liner. Destruction on depressurization may be more severe if flashing occurs, but the temperature is likely to be much less severe. Greater thicknesses of insulation are required because of the better heat transfer properties of liquids.

3.7.3 Cooling

The cooling system (Figure 4) consists of systems of bright mild steel square section pipes, welded to the liner at 6 inch centres. Alternate pipes are connected to completely independent water circulation systems to ensure reliability of supply. Headers are normal round section pipe.

The primary water ciruit is closed, demineralized, and held oxygen free. It gives up its heat through exchangers to a secondary circuit in parallel with the main condenser cooling circuit.

For the reference design of reactor the temperature of the concrete due to radiation heating would rise 15 to 20°C above the liner temperature. With only one cooling circuit operating, there is a 20°C rise along the liner, and with both operating, 5°C. With cooling water in the walls at 30°C, the concrete temperature should normally be not more than 55°C, and never more than 70°C.

3.7.4 Shielding

Shielding must be provided to limit the irradiation of the mild steel liner so that its ductility at operating temperatures will not be significantly reduced. This must be checked for each design.

3.7.5 Penetrations

Where access is required for control rods, circulators, steam pipes, etc., two problems arise. The first is how to seal against the pressure, and the second, how to compensate for the concrete removed. The solution adopted employs a low carbon steel lining tube, welded to the vessel liner and carried out through the wall to a pressure flange. If the tube is thicker than the vessel liner, the latter is thickened up around the penetration.

The lining tube should also be heavily anchored to the concrete of the wall, because cooling tubes are required around it, and they must not be sheared off by relative movement. If the tube did not require cooling, it could be left free to creep in the concrete, being anchored only on the inner end, and thus avoid the axial compressive strain otherwise applied to it. Inside cooling would permit this, but make insulation difficult. However, complete anchoring should be quite satisfactory, because the really significant compressive strains are circumferential.

To achieve strain compatibility with the concrete, and thus not introduce stress concentrations, the penetration liner thickness should be one twelfth of its diameter. But to withstand the concrete compression in the wall without

deforming when the vessel is depressurized, its thickness should be one seventh to one eighth of its diameter. A compromise thickness of one tenth of the diameter was chosen, as unlikely to cause excessive stress concentration, and with cooling tubes and stiffening ribs, unlikely to deform. This is examined in Appendix 9. Tensile loading of penetration liners under test pressure conditions is shown in Appendix 10 to be of no significance.

The size of penetrations must be limited to prevent a too rapid depressurization in the event of failure, as well as not to interfere too much with tendon arrangement.

Large penetrations should if possible, be kept away from highly stressed regions. From the point of view of vessel design, the most favourable situation seems to be through the end slabs, away from the high shear stresses near the edge, and if possible, centred on the radius of contraflexure. However, results of Campbell-Allen and Low (1967) suggest that slab failure may initiate not far from this location, but this needs to be proved by further experiment.

4. COSTING

In Appendix 11, the derivation of equations giving the cost of the different parts of the vessel, is discussed. In most cases cost coefficients are employed, which can be given different values, depending on where, and how, the vessel is to be built.

The reason for deriving such equations is that they can be programmed for a computer together with the design equations (for example, the programme VESSEL) and produce a complete cost break-down for as many design variations as required. If care is taken, such a programme may be used as part of a complete reactor optimization code (for example the programme NUROSYS). This was done for optimization of the reference design. (Ebeling and Hayes 1967).

The costing used for the reference design in programme VESSEL, was also used to show the effect on cost of varying different design parameters. This is discussed in Section 5.

For the reference design 200 MWe H.T.G.C.R. (CO_2, 1000 p.s.i.g., 320°C, contained boilers, penetrations for boiler tubes and circulators as well as control and fuel handling), the following cost breakdown was obtained. The absolute values should not be taken too seriously, but the relative values point up the expensive aspects of such P.C.P.V. designs.

		$A 10^3	per cent	$A 10^3	per cent
Concrete		293	9		
Reinforcement		112	4	405	13
Tendons	- cylindrical	262	9		
	- vertical	138	4		
	- end slab	121	4		
	- place and tension	30	1	551	18
Walls	- liner	192	6		
	- insulation	286	9		
	- cooling	36	1	514	16
Pentrations	- liners	1,030	33		
	- insulation	363	12		
	- cooling	70	2	1,463	47
Monitoring		108	3	108	3
External cooling circuit		93	3	93	3
		3,134	100	3,134	100

The following is a different grouping of some of the items:

Liners	- wall	192	6		
	- penetrations	1,030	33	1,222	39
Insulation	- wall	286	9		
	- penetrations	363	12	649	21
Cooling	- wall	36	1		
	- penetrations	70	2		
	- external circuit	93	3	199	6

General conclusions from these breakdowns are:

1. Concrete, with its reinforcement and cooling, is not expensive - less than 20 per cent of total cost.
2. Tendons, also, are not expensive - less than 20 per cent of total cost.
3. Lining of the wall and penetrations accounts for nearly 40 per cent of the total cost.

4. Insulation of the wall and penetrations, accounts for over 20 per cent of the total cost.

5. The most surprising result, is that penetrations (lining, insulation and cooling) account for nearly 50 per cent of the total cost.

When examining the cost trends of Figure 5, the large effect on costs of 'secondary' items such as penetrations, liners, insulation, etc., must be borne in mind.

5. DESIGN LIMITS AND COST TRENDS OF P.C.P.V.s

In the preceding sections, the practical requirements for, and properties of, P.C.P.V.s (for H.T.G.C.R.s in particular) have been briefly examined. Idealized but conservative equations have been set up to describe the design of the type of cylindrical vessel chosen. The behaviour of these equations is now examined to obtain an understanding of the limits of the design, and of the economic performance of P.C.P.V.s. This is essential for their application to different reactor systems.

5.1 The Controlling Equations

The following 12 equations are taken from the preceding sections. Given concrete stress limits (f_c and f_t), tendon breaking load (T_u), vessel pressure (p_w, γ, β), diameter (d_i), and number of ribs (r), we can determine uniquely the wall and end slab thicknesses (α, t) and tendon arrangement parameters (n_z, n_b, X, θ_r, S_hS_v).

$$f_c = 2\, p_{s(ten)}\, \frac{\alpha^2}{\alpha^2-1} \qquad .....5.1$$

$$f_t = 2\, p_{s(td)}\, \frac{\alpha^2}{\alpha^2-1} - \gamma\, p_w\, \frac{\alpha^2+1}{\alpha^2-1} \qquad .....5.2$$

$$n_b = 66\beta p_w\, d_i/T_u \qquad .....5.3$$

$$p_{s(ten)} = 0.62\, T_u\, \epsilon_1\, n_b/66\alpha\, d_i \qquad .....5.4$$

$$p_{s(td)} = 0.58\, T_u\, \epsilon_2\, n_b/66\alpha\, d_i \qquad .....5.5$$

$$\epsilon_1 n_z = 1+e^{-\mu(\frac{2\pi}{r}-\theta_r)} + e^{-\mu(\frac{2\pi}{r})} + e^{-\mu(\frac{4\pi}{r})} + \text{ + } e^{-\mu(\frac{6\pi}{r}-\theta_r)} + e^{-\mu(\frac{6\pi}{r})} + \text{ ..... to } n_z \text{ terms.} \qquad .....5.6$$

$$\epsilon_2 n_z = e^{-\mu(\frac{\pi}{r}-\frac{\theta_r}{2})} + e^{-\mu(\frac{\pi}{r}-\frac{\theta_r}{2})} + e^{-\mu(\frac{3\pi}{r}-\frac{\theta_r}{2})} + \text{ + } e^{-\mu(\frac{5\pi}{r}-\frac{\theta_r}{2})} + e^{-\mu(\frac{5\pi}{r}-\frac{\theta_r}{2})} + e^{-\mu(\frac{7\pi}{r}-\frac{\theta_r}{2})} + \text{ ..... to } n_z \text{ terms.} \qquad .....5.7$$

$$\cos\theta_r = (12\alpha d_i - X)/(12\alpha d_i + X) \qquad .....5.8$$

$$X = (n_b - 1)\, 11 + 16 \qquad .....5.9$$

$$S_hS_v = 1.74\, T_u/(f_c + f_t) \qquad .....5.10$$

$$t \geq (d_i/2)\sqrt{1.275\beta\, p_w/(f_c - f_t)} \qquad .....5.11$$

$$t \geq 0.375\beta p_w d_i\left[\left(\frac{0.435T_u}{S_hS_v} + \frac{\beta p_w}{4} - f_t\right)^2 - \left(\frac{0.435T_u}{S_hS_v} - \frac{\beta p_w}{4}\right)^2\right]^{-\frac{1}{2}} \qquad .....5.12$$

5.2 Direct Solution on Computer

Solution of Equations 5.10, 5.11 and 5.12 for the end slab dimensions is obvious. Solution of Equations 5.1 to 5.9 for the cylinder wall is more indirect. Neglecting the handling of some of the inherent limits yet to be described, the following steps are used for values of r from 2 to 7.

1. On the approximation that $\epsilon_1 = \epsilon_2$, α is obtained from Equations 5.1, 5.2, 5.4 and 5.5 as:

$$\alpha = \left(\frac{(0.937f_c - f_t) + \gamma p_w}{(0.937f_c - f_t) - \gamma p_w}\right)^{\frac{1}{2}}.$$

2. n_b (from Equations 5.3) and α are then used in Equations 5.8 and 5.9 to obtain X and θ_r (note that n_b is taken to the nearest greater integer).

3. Equations 5.6, 5.4 and 5.1 are then solved to give new values of α, for values of n_z ranging from 5.2 to 5.10.

4. Equations 5.7, 5.5 and 5.2 are then solved to give further values of α, for values of n_z ranging from 2 to 10.

5. The integer value of n_z which gives the most nearly corresponding values of α is then chosen and the mean α value obtained.

6. This process is then repeated as often as necessary from step 2, to obtain an accurate result. Few iterations are required, because X and θ_r are not very sensitive to change of α, and the approximation $\epsilon_1 = \epsilon_2$ is usually quite good.

It can be noted here that the solution for α of step 4 above is an equation:

$$\alpha = \left(0.58\epsilon_2\beta p_w \pm \sqrt{(0.58\epsilon_2\beta p_w)^2 - (\gamma^2 p_w^2 - f_t^2)}\right) \Big/ (\gamma p_w + f_t) \quad ,$$

and the negative sign under the root sign imposes the limit that:

$$(0.58\epsilon_2\beta)^2 \geq \gamma^2 - (f_t/p_w)^2 \quad .$$

If normally $\beta = 2.75$, $\gamma = 1.33$, $\epsilon_2 \approx 0.85$ and $f_t/p_w = 0.2$, then variation of β, γ or ϵ alone is restricted so that:

$$\beta \not< 2.67, \quad \gamma \not> 1.37, \quad \epsilon_2 \not< 0.82 \quad .$$

5.3 Tendon Arrangement Effects

Figure 5 shows a cost advantage from using as many anchor ribs as practicable. Six seems a very good compromise, because more ribs restrict penetrations, tendon handling, etc.,

The following table (for reference design conditions) shows that for numbers of ribs greater than four, $\epsilon_1 = \epsilon_2$ to better than 1 per cent accuracy. The range of n_z values is restricted for small values of r, because of the limit on ϵ_2 described in Section 5.2. The fact that ϵ_1 and ϵ_2 are indistinguishable for larger values of r, means that there is negligible variation in the inward tendon pressure around the circumference of the cylinder.

VALUES OF ϵ_1 AND ϵ_2 FOR VARIOUS TENDON ARRANGEMENTS

Ribs r	ϵ	Tendon Arrangement Parameter n_z								
		2	3	4	5	6	7	8	9	10
2	ϵ_1	81	72							
	ϵ_2	79	66							
3	ϵ_1	88	80	73						
	ϵ_2	87	77	72						
4	ϵ_1	92	86	80	75					
	ϵ_2	92	84	79	73					
5	ϵ_1	95	89	84	80	75				
	ϵ_2	95	88	84	79	75				
6	ϵ_1	97	92	88	83	80	76			
	ϵ_2	97	91	88	83	80	76			
7	ϵ_1	98	93	90	86	83	80	77	73	
	ϵ_2	98	93	90	86	83	79	77	73	

5.4 Analytic Solutions

Equations 5.1, 5.2, 5.4 and 5.5 may be solved to give:

$$\alpha = \left(\frac{\left(\frac{\epsilon_2}{1.07\epsilon_1} f_c - f_t\right) + \gamma p_w}{\left(\frac{\epsilon_2}{1.07\epsilon_1} f_c - f_t\right) - \gamma p_w} \right)^{\frac{1}{2}}$$

Thus if ϵ_1 can be put equal to ϵ_2, the cylinder wall thickness ratio α is determined by the test pressure and allowable concrete stresses, without any reference to ultimate pressure conditions. Figure 6 shows α as a function of p_w for $\epsilon_1 = \epsilon_2$, $\gamma = 1.33$, $f_c = 2500$ p.s.i. and $f_t = -200$ p.s.i.

that is, $\alpha = \left((2540 + 1.33\, p_w) \Big/ (2540 - 1.33\, p_w)\right)^{\frac{1}{2}}$.

Thus unless higher concrete stresses are permitted, or a lower test pressure, the fully elastic design criterion (based on the Lamé equation) limits practicable working pressures to about 1500 p.s.i.

Taking the above value of α (for $\epsilon_1 = \epsilon_2 = \epsilon$), and considering only the case of $f_c = 2500$ p.s.i. and $f_t = -200$ p.s.i., Equations 5.1 or 5.2, with Equation 5.3 for ultimate conditions, give:

$$\epsilon = \frac{2500\,\gamma}{0.62\,\beta}\left(2540^2 - (\gamma p_w)^2\right)^{-\frac{1}{2}} \quad .$$

This equation is also plotted in Figure 6, and if it is remembered that ϵ cannot be > 1, it is clear that more circumferential tendons are necessary for $p_w \geq 1230$ p.s.i. than are required by ultimate conditions (Equation 5.3). Then if Equation 5.3 is neglected:

$$\epsilon\, n_b = d_i/(2.78\sqrt{(2540/\gamma p_w)^2 - 1}) \quad .$$

If ϵ is put equal to 1, a value for n_b follows, which can be taken to the next higher integer value, and ϵ adjusted to suit by varying n_z (r is fixed). This minimum value of n_b for $\gamma = 1.33$ is also shown in Figure 6 as a multiple of d_i for values of $p_w > 1230$. Thus for these high pressures, the number of circumferential tendons (that is, n_b) increases very rapidly. For pressures < 1230, n_b/d_i is plotted from Equation 5.3, and is dependent on β. Above 1230, n_b/d_i depends not on β but on γ.

5.5 Variation of Tendon Working Stress

It has been assumed that the working prestress of tendons will be 60 per cent of the minimum breaking load. In the programme VESSEL, the effect of varying this prestress is examined by the use of a parameter ω, given by:

$$\omega = \frac{\text{actual tendon working load}}{0.60 \times \text{minimum tendon breaking load}}$$

This parameter ω appears as a multiple of T_u in Equations 5.4 and 5.5, and Equation 5.10. From Equation 5.10, the effect of reducing the working load of the end slab tendon is to increase their number, and hence cost. The equation for α (Section 5.4) cancels out ω. However, computer solutions, taking separate account of ϵ_1 and ϵ_2, show a decrease in α with decrease in ω. But the overall effect on cost (Figure 5) shows that the increase in tendon cost, especially end tendons, is greater than the decrease in concrete cost.

Above 1230 p.s.i. working pressure (refer Figure 6) n_b is no longer determined by ultimate conditions, but is given by:

$$\epsilon n_b = \frac{106.4\, f_c\, d_i}{\omega\, T}\left[\left(\frac{0.937\, f_c - f_t}{\gamma\, p_w}\right)^2 - 1\right]^{-\frac{1}{2}} \quad .$$

Here the number of tendons n_b is inversely dependent on their working load w. The pressure above which this is so, is also dependent on ω. That is:

$$\text{transition } p_w = \left[\left(\frac{0.937 f_c - f_t}{\gamma}\right)^2 - \left(\frac{1.61\, f_c}{\beta\,\omega}\right)^2\right]^{\frac{1}{2}} .$$

The effect of this (for $f_c = 2500$, $f_t = -200$, $\gamma = 1.33$ and $\beta = 2.75$) is seen in the following table:

ω	0.8	0.9	1.0	1.1	1.2
Transition p_w (p.s.i.)	567	1010	1230	1375	1480

5.6 Sensitivity of Solutions

The curves of Figure 7 illustrate some of the unexpected trends of the design equations. They also show that quite small variations of tendon parameters can make very great changes in the solution for wall thickness ratio α. (They are solutions of Equations 5.1, 5.2 and 5.3 for reference design conditions, and $\epsilon_1 = \epsilon_2 = 0.90$).

The curves of Figure 5 are drawn smooth, but solutions for some of the variables are quite scattered owing to the need for n_z and n_b to be integers. However, the trends are quite clear

5.7 Other Trends

Figure 5 shows variation of cost as selected parameters are varied one at a time about their reference design values. These curves show the cost sensitivity of the different parameters, for example, variation of d_i has much more effect than variation of H; variation of p_w, than variation of p_{td} or p_u (that is, γ, β) variation of concrete stress, than tendon parameters (that is, r, ω).

The variation of cost with ultimate pressure p_u (that is, β) is worth comment. Increase in β increases end slab thickness but decreases cylinder wall thickness. The relative effectiveness of these variations produces a cost minimum for $\beta \sim 2.65$. The dependence of end slab thickness on β, results from the conservative safety criterion adopted. If slab testing were to justify a relaxation of this criterion, cost variation with β would be modified.

6. NOTATION

Several recurring subscripts are as follows:

- td - test design
- ten - at tensioning
- u - ultimate
- w - working

The following symbols appear either as given, or with the above subscripts:

A	-	rib width at diameter D_o	ft
A	-	cross sectional area of tendon	in^2
C	-	anchor spacing	inch
C	-	cost	$A
D_o	-	outside diameter of vessel between ribs	ft
E	-	Youngs modulus	p.s.i.
F_c	-	radial force per unit tendon length	lb/ft
F_c	-	radial force on rib, per unit circumference	lb/ft
H	-	inside vessel height	ft
K	-	friction factor for 'straight' tendons	ft^{-1}
L_c	-	mean circumferential tendon length	ft
L_e	-	length of end slab tendons	ft
L_v	-	length of vertical tendons	ft
M	-	bending moment	
R	-	radius of curvature	
S	-	shearing force per unit circumference	lb/ft
S	-	cost coefficient	$A per -
S_h	-	horizontal pitch of end slab tendons	inch
S_v	-	vertical pitch of end slab tendons	inch
T	-	tendon tension	lb
T_{ea}	-	effective average hoop tendon tension	lb
T_u	-	ultimate tendon tension	lb
T_v	-	vertical tendon tension	lb
T_θ	-	hoop tendon tension at θ	lb
T_{θ_o}	-	hoop tendon tension at end of curvature	lb
V	-	volume of reinforcement steel	in^3
X	-	radial space occupied by a band of tendons	inch
a	-	width of outer face of rib	ft
a	-	half side of anchor reinforcement cube	inch
b	-	width of band of tendons between centre lines	inch
c	-	tendon edge clearance	inch
d_i	-	vessel inside diameter	ft
d_o	-	tendon mean pitch diameter	ft
d_p	-	diameter of penetration	ft

f_c	-	design compressive stress for concrete	p.s.i.
f_c'	-	concrete cylinder strength - uniaxial loading	p.s.i.
f_c''	-	concrete failure strength - biaxial loading	p.s.i.
f_h	-	stress at horizontal centre line	p.s.i.
f_v	-	stress at vertical centre line	p.s.i.
f_t	-	design tensile stress for concrete	p.s.i.
h	-	height of a tendon 'zone'	inch
n_b	-	number of tendons in a 'band'	-
n_e	-	number of tendons in each end slab	-
n_h	-	number of hoop tendons	-
n_h	-	number of helical tendons	-
n_L	-	number of layers of helical tendons	-
n_v	-	number of vertical tendons	-
n_z	-	number of hoop tendon layers in a zone	-
p	-	pressure	p.s.i.
p_{cc}	-	concrete cracking pressure	p.s.i.
p_i	-	internal pressure	p.s.i.
p_o	-	external pressure	p.s.i.
p_s	-	prestress equivalent pressure	p.s.i.
r	-	number of ribs	-
r	-	radius of end slab	ft
r_o	-	outside radius of end slab	ft
t	-	thickness of end slab to resist pressure	ft
t_p	-	penetration liner thickness	inch
t_s	-	thickness of end slab with inside shielding	ft
v	-	vertical distance from neutral axis of end slab	ft
ω	-	tendon working stress multiplier	ft
α	-	tendon pitch diameter multiplier (d_o/d_i)	-
β	-	ultimate pressure multiplier (p_u/p_w)	-
γ	-	test design pressure multiplier (p_{td}/p_w)	-
Δ	-	tendon extension	-
θ_r	-	angle subtended by a rib	radians
θ_w	-	wrap angle of hoop tendons	radians
ϕ	-	angle from rib	radians
μ	-	friction factor for curved tendons	$radians^{-1}$
σ_b	-	bending stress	p.s.i.
σ_c	-	circumferential stress	p.s.i.
σ_d	-	direct stress	p.s.i.

σ_h	-	horizontal stress	p.s.i.
σ_i	-	circumferential stress on inside face	p.s.i.
σ_n	-	principal stress	p.s.i.
σ_{ps}	-	prestress	p.s.i.
σ_r	-	radial stress	p.s.i.
σ_s	-	shear stress	p.s.i.
σ_v	-	vertical stress	p.s.i.
σ_1, σ_2, σ_3	-	principal compressive failure stresses	p.s.i.

7. REFERENCES

Beer, F. J. (1964). - Discussion on Waters and Barrett (1963); J. Brit. Nucl. Energy Soc., April 1964.

Bellamy, C. J. (1961). - Strength of concrete under combined stress; J. Am. Conc. Inst., October 1961.

Campbell-Allen, D., Hayes, J. E., Low, E. W. E., Spencer, A. (1967). - P.C.P.V. for an Australian H.T.G.C.R.; Paper 7h. Inst. Civil Eng. Conference on Prestressed Concrete Pressure Vessels, London. 1967.

Ebeling, D. R., and Hayes, J. E. (1967). - The engineering design and analysis of a beryllia-moderated pebble bed reactor. Paper prepared for the Institution of Engineers. (Australia).

Houghton-Brown, A., Hay, J. D., Hyde, R. B., and Sprace, T. W. (1964). - P.C.P.V.s ref. Oldbury; A/Conf. 28/P/140.

Houghton-Brown, A., Harris, J. D., Taylor, R. S., Phillips, R. S., Gilli, P. V., Lakin, R. W. (1964). - Separate contributions, in order, to discussion on Waters and Barrett (1963); J. Brit. Nucl. Energy Soc., April 1964.

Kaiser Engineer. (1962). - Guide to nuclear power cost evaluation. TID-7025.

Lamiral, G., Laurent, L., Bonnelle, R., Beaujoint, H. and Faurot, A. (1964). - P.C.P.V.s for French gas type reactors; A/Conf. 28/P/52.

Lin, T. Y. (1963). - Design of Prestressed Concrete Structures; J. Wiley.

Timoshenko, S. (1956). - Strength of Materials II: Van Nostrand.

Taylor, R. S., and Williams, A. J. (1964). - Design of P.C.P.V. ref. Wylfa; A/Conf. 28/P/141.

Troxell, G. E., and Davis, H. E. (1956). - Composition and Properties of Concrete; McGraw Hill.

Warner, P. C. (1964). - Discussion on Waters and Barrett (1964); J. Brit. Nucl. Energy Soc., April 1964.

Waters, T. C., and Barrett, N. T. (1963). - P.C.P.V.s for nuclear reactors; J. Brit. Nucl. Energy Soc., July 1963.

APPENDIX 1

INCREASED STRENGTH UNDER BIAXIAL LOADING

From tests on hollow concrete cylinders (Bellamy 1961) the following relations may be used:

$$\sigma_1 = f_c' + 0.75\,\sigma_2 \quad \text{for biaxial loading,}$$

$$\sigma_1 = f_c' + 2.9\,\sigma_2 \quad \text{for triaxial loading,}$$

where σ_1, σ_2 and σ_3 are the principal compressive stresses at failure. For biaxial loading $\sigma_3 = 0$ and for triaxial, $\sigma_3 = \sigma_2$.

Bellamy's results for triaxial loading agree with results from Troxall and Davis (1956), and results they quote from other sources that even higher strengths are likely. Thus Bellamy's results for biaxial loading can be inferred to be accurate also, and they are particularly useful here because the test arrangement was designed for a failure stress occurring on the inside wall of a cylinder externally loaded.

Application to Cylinder Wall

A maximum circumferential stress σ_c, occurs on the inside face of the wall, for the condition of no internal pressure. By the design method outlined in this paper:

$$\sigma_c = 1.2\,p_u\,\alpha/(\alpha^2 - 1) = \sigma_1 \quad .$$

The corresponding vertical stress, assumed uniform over the cross section, is given by:

$$\sigma_v = 0.6\,p_u/(\alpha^2 - 1) = \sigma_2 \quad .$$

The radial stress on the inside face of the wall is zero, giving biaxial loading, and, dividing, we have:

$$\sigma_1/\sigma_2 = 2\alpha \quad .$$

For the range $1.5 < \alpha < 2$

$$3 < \sigma_1/\sigma_2 < 4 \quad .$$

The failure stress f_c'', is given by:

$$f_c'' = f_c' + 0.75\,f_c''/(3 \text{ to } 4)$$

$$= (1.23 \text{ to } 1.33)\,f_c'$$

$$= 7{,}380 \text{ to } 8{,}000 \text{ p.s.i. for } f_c' = 6000 \text{ p.s.i.}$$

continued...

APPENDIX 1 (Continued).

If we further make the reasonable assumption that any cause leading to local failure will affect the total vertical and circumferential stresses in the same proportion as the primary stresses, we can then use a design stress:

$$f_c = \frac{1}{3} f_c''$$

$$= 2{,}500 \text{ p.s.i. say.}$$

Application to End Slabs

Figure 8 shows the combination of bending stresses and prestress along a radius of an end slab. At the centre of the slab, the limiting compressive stress is equal in all horizontal directions. At the edge the limiting circumferential stress is less than half the radial stress. Applying Bellamy's relationship for biaxial stress, and a factor of safety of three, as for the cylinder walls, the plotted permissible compressive design stresses are obtained.

Because the conditions of stress and mode of failure in thick slabs of this type are not fully understood, an arbitrary figure of $f_c = 2{,}500$ p.s.i. was used in design rather than the variable values of f_c'' which are theoretically applicable. Thus although the limiting conditions for design are taken in the centre of the slab where stresses are highest, it can be seen that the margin to failure may actually be slightly less at the edge.

APPENDIX 2

SLAB PRESTRESS

For the arrangement of tendons seen in Figure 1 it can be shown that the compressive stress due to the pre-tensioning of the tendons, is given by:

$$\sigma_{ps} = 1.5\, T/S_h\, S_v \quad . \qquad .....(1)$$

This stress is found on any vertical cross section of the slab through the pressure loaded area, regardless of its orientation with respect to the tendon systems. It is assumed that the tendons are spaced from top to bottom of the slab, at pitch S_v, that is, any concrete added on the inside for shielding of the tendons thicker than $\frac{1}{2} S_v$, is neglected.. It is also assumed that each tendon system fully covers the pressure loaded area of the slab.

For a number of tendon systems other than three, the same type of formula applies, but with a different multiplier (for example, for 2 systems at 90°, $\sigma_{ps} = 1.0\, T/S_h\, S_v$).

Allowing for tendon tension losses as described in Appendix 5, but neglecting friction (on the ground that the tendons will be placed in straight smooth tubes, without "wobble"), we have:

$$\sigma_{ps(td)} = 0.93\, T_u/S_h\, S_v \qquad .....(2)$$

$$\sigma_{ps(u)} = 0.87\, T_u/S_h\, S_v \quad . \qquad .....(3)$$

The elastic bending stresses derived in Appendix 3, are plotted against the radius of the slab in Figure 8. The design limits are that the tensile stress at the centre of the outer surface of the slab shall not exceed f_t and that the compressive stress at the centre of the inner surface of the slab shall not exceed f_c.

$$\sigma_{ps(u)} - \sigma_{r(u)\ (r=o)} = f_t \qquad .....(4)$$

$$\sigma_{ps(u)} + \sigma_{r(u)\ (r=o)} = f_c \quad . \qquad .....(5)$$

Only ultimate conditions are considered because although $\sigma_{ps(td)}$ is 7 per cent. greater than $\sigma_{ps(u)}$, p_u and hence $\sigma_{r(u)}$ are respectively 20 per cent. greater than p_{td} and $\sigma_{r(td)}$.

APPENDIX 3

BENDING OF END SLABS

A fair estimate of the bending stresses in thick slabs may be obtained from thin slab formulae . Such formulae given, for example, by Timoshenko (1956) are inaccurate only because they do not take full account of shear stress, and thus do not correctly estimate deflection. For circular slabs, with Poisson's ratio = 0.2 they reduce to:

$$\sigma_r \quad \frac{8t^2}{3p} = Z\, r_o^2 - 3.2\, r^2 \qquad .....(1)$$

$$\sigma_c \quad \frac{8t^2}{3p} = Z\, r_o^2 - 1.6\, r^2 \quad , \qquad .....(2)$$

where Z is a constant, whose value depends on the degree of edge restraint. 'Clamped' and 'simply supported' cases set the limits:

$$1.2 < Z < 3.2 \quad .$$

Tests on slabs of similar proportions to these have been performed at Sydney University by Campbell-Allen and Low (1967). The edge restraint of their slabs appears to be a realistic approximation for slabs forming part of a vessel of the type proposed here. Strain gauge readings on the three slabs tested, all showed a radius of contraflexure of about 8 inches for a slab radius of 11 inches. In the equation for σ_r above, putting $r_o = 11$ and $r = 8$, for $\sigma_r = 0$, gives $Z = 1.7$. For the slabs to be considered, then, Equations 1 and 2 become:

$$\sigma_r \quad \frac{8t^2}{3p} = 1.7\, r_o^2 - 3.2\, r^2 \qquad .....(3)$$

$$\sigma_c \quad \frac{8t^2}{3p} = 1.7\, r_o^2 - 1.6\, r^2 \quad . \qquad .....(4)$$

These formulae can now be used to obtain the bending stresses of the composite slabs. They cannot be used to calculate deflection.

APPENDIX 4

SHEARING OF END SLABS

Final failure of some test slabs (Campbell-Allen and Low 1967; Warner 1964) of the type considered here has been by shear. The following simple analysis provides a conservative criterion for slab thickness, to avoid such failure.

The shearing force per unit circumferential length at radius r, is given by:

$$S = p\,\pi\, r^2/2\,\pi\, r = \tfrac{1}{2}\, pr \quad . \qquad .....(1)$$

The corresponding shear stress is given by:

$$\sigma_s = \frac{3S}{2t^3}\,[\, t^2 - 4v^2\,]$$

$$= \frac{3pr}{4t^3}\,[\, t^2 - 4v^2\,] \quad , \qquad .....(2)$$

where v is the vertical distance from the neutral axis. The maximum value occurs on the neutral axis where v = 0.

$$\sigma_{s(max)} = 3\, pr/4t \quad . \qquad .....(3)$$

This shear stress does not cause failure as such, but in conjunction with the bending stresses, and prestress, may produce a tensile principal stress leading to failure.

Principal stresses in a vertical radial plane are given by:

$$\sigma_n = \frac{\sigma_h + \sigma_r}{2} \pm \sqrt{\left(\frac{\sigma_h - \sigma_v}{2}\right)^2 + \sigma_s^2} \quad . \qquad .....(4)$$

It can be shown that the limiting value of σ_n occurs at the outside radius of the slab, only slightly displaced from the neutral axis. Within the accuracy with which the material properties are known, σ_n may be taken on the neutral axis. Then because the bending stresses there are zero:

$$\sigma_h = \sigma_{ps}$$

$$\sigma_v = p/2$$

$$\sigma_s = 3\, p\, r_o/4t \quad .$$

To ensure integrity of the slab up to ultimate pressure, σ_n must not exceed f_t for ultimate values of σ_h, σ_v and σ_s.

Continued...

APPENDIX 4 (Continued)

$$f_t = \frac{\sigma_{s(u)}}{2} + \frac{p_u}{4} - \left[\left(\frac{\sigma_{ps(u)}}{2} - \frac{p_u}{4} \right)^2 + \left(\frac{3\, p_u\, r_o}{4t} \right)^2 \right]^{\frac{1}{2}} \quad \ldots\ldots(5)$$

From Equation 3 of Appendix 2, put $\sigma_{ps(u)} = 0.87\ T_u/S_u\ S_v$, and solve for the limiting value of t.

$$t = 0.75\ p_o r_o \left[\left(\frac{0.435 T_u}{S_h\ S_v} + \frac{p_u}{4} - f_t \right)^2 - \left(\frac{0.435 T_u}{S_h\ S_v} - \frac{p_u}{4} \right)^2 \right]^{-\frac{1}{2}} .$$

$\ldots\ldots(6)$

APPENDIX 5

TENDON FRICTION AND RELAXATION

After a tendon is tensioned, it relaxes due to the following causes:

(1) set in the anchor,

(2) elastic shortening of the concrete due to the subsequent tensioning of more tendons,

(3) shrinkage of the concrete due to further curing and drying,

(4) creep of both concrete and steel.

Relaxation is in part allowed for by overstressing when tensioning. For the tendons we are considering, prestressing up to 85 per cent. of ultimate is usually permitted and the working stress up to 60 per cent. Note, however, that this 60 per cent. does not include stress resulting from application of load.

Another very important cause of reduced tendon tension, is friction in the anchors and tendon ducts. This, and the relaxations mentioned above, will now be considered in turn.

Tendon Friction

If T_o is the tension in the tendon at the jack, and T the tension at a distance x along the rope duct, nominally straight:

$$T = T_o\, e^{-Kx} \quad \text{where } K = 10^{-3}\ ft^{-1} .$$

For a curved duct, turning through an angle θ :

$$T = T_o\, e^{-\mu\theta} \quad \text{where } \mu = 0.20 \text{ to } 0.25 .$$

The value assumed for μ in this design is 0.20. This is a realistic value for smooth steel tubes, and tendons coated with tar or a similar material. For a final design, the economics of using a higher μ and more tendons, but dispensing with lubricant, could be examined.

Friction loss in the jack is normally assumed to be about 5 per cent. and it is compensated for by going to a higher jacking force. The effects of all such extra jack pressures are checked by tendon elongation readings.

Anchor Set

Depending on the type of anchor, the wedges may set in $\frac{1}{4}$ inch to $\frac{3}{4}$ inch when the load comes on them. This relaxes the stress in the tendon to a degree determined by the duct friction, as will be seen.

Continued...

APPENDIX 5 (Continued)

If, in Figure 9, A is the cross-sectional area of the tendon, the strain at tension T_θ is given by:

$$S_\theta = \frac{T_\theta}{AE}$$

The elongation $\delta\Delta$ due to this strain on an increment of length $R\delta\theta$ is given by:

$$\delta\Delta = S_\theta \, R \, \delta\theta = \frac{RT_\theta}{AE} \, \delta\theta$$

The total elongation at the anchor is given by:

$$\Delta = \frac{R}{AE} \int_0^{\theta_m} T_\theta \, d\theta \quad ,$$

where θ_m defines the mid-point of the tendon. This assumes tensioning from both ends. Remembering that $T_\theta = T_o e^{-\mu\theta}$, we have:

$$\Delta = \frac{RT_o}{AE} \int_0^{\theta_m} e^{-\mu\theta} \, d\theta$$

$$= \frac{RT_o}{AE\mu} \, (1 - e^{-\mu\theta_m})$$

Similarly, for straight rope of length x :

$$\Delta = \frac{T_o}{AEK} \, (1 - e^{-Kx})$$

Refer now to Figure 10, and consider the effect of an anchor set δ on a tendon tensioned at the jack to T_o. Due to δ, T_o will now relax to T'_o. Also, along the tendon, at a distance L say, there will be a maximum tension T_L unaffected by the relaxation due to δ. T_L is related to both T_o and T'_o as follows, assuming for the moment that the tendon is 'straight':

$$T_L = T_o e^{-KL}$$

$$T'_o = T_L e^{-KL}$$

This second equation is as for the tendon anchored at T'_o and tensioned at L.

Continued...

APPENDIX 5 (Continued)

The value T_L is further defined because:

$$\Delta L, \text{ which } = \frac{T_L}{AEK} \, (1 - e^{-KL})$$

is also equal to δ

We then have:

$$\delta = \frac{T_o}{AEK} \, (1 - e^{-KL}) \, e^{-KL}$$

$$T_L = T_o e^{-KL}$$

$$T'_o = T_o e^{-2KL} \quad .$$

These relations are plotted in Figure 14. For real anchor set values, the resulting relaxation is confined to a distance not greater than 5 to 10 feet from the anchor and relaxation at the point of resulting maximum tension will be less than 1 per cent. Thus for simplicity the resulting maximum tension T_L can be assumed to occur at the edge of the rib and to be $\leq 0.99 \, T_o$.

Elastic Shortening of Concrete and Steel Relaxation

Elastic shortening of the concrete is immediately effective and as shown by Lin (1963) results in about 3 per cent. relaxation, irrespective of the number of tendons.

Steel relaxation, or creep, occurs in about 3 days and can be considered effective immediately. It also results in about 3 per cent. relaxation.

Concrete Creep and Shrinkage

Concrete creep and shrinkage contribute strains of 4.5×10^{-4} and 2.0×10^{-4} respectively, subject however, to much variation. In both cases, half the strain occurs in the first month and three-quarters in the first 6 months. The total eventual strain of 6.5×10^{-4}, is equivalent to a stress relaxation of 9 per cent. (for Dyform strand initially tensioned to 80 per cent. of ultimate, that is, $6.5 \times 10^{-4} / 73.4 \times 10^{-4}$).

Effective Single Rope Tensions

We have seen that the maximum tension in a tendon can be assumed to occur

Continued...

APPENDIX 5 (Continued)

at the edge of the rib, where curvature begins. Thus this value $T_L = 0.99\ T_o$ can also be called T_{θ_o}.

If we assume that the vessel will not be commissioned for at least 6 months after tensioning, then T_{θ_o} at six months $= 0.60\ T_u$. T_o at tensioning will then be:

$$T_{o(ten)} = 0.60\ T_u \times \underset{\text{(concrete shortening)}}{\frac{1}{0.97}} \times \underset{\text{(steel relaxation)}}{\frac{1}{0.97}} \times \underset{\text{(creep and shrinkage)}}{\frac{1}{0.93}} \times \underset{\text{(anchor set)}}{\frac{1}{0.99}}$$

$$\approx 0.70\ T_u \quad .$$

Allowing 5 per cent. for anchor friction, the necessary jacking force is still well below the $0.85\ T_u$ permitted.

For consideration of concrete crushing due to prestress, assume that the jacking is spread over a few months and that 4 per cent. relaxation can be assumed for concrete creep and shrinkage. Other relaxations will be fully effective.

$$\text{Thus } T_{\theta_o(ten)} = 0.60\ T_u\ \frac{0.96}{0.93}$$

$$= 0.62\ T_u \quad .$$

On the other hand, it must be assumed that test pressure might be applied when full concrete relaxation has occurred.

$$\text{Thus } T_{\theta_o(td)} = 0.60\ T_u\ \frac{0.91}{0.93}$$

$$= 0.587\ T_u, \quad \text{say,} \quad 0.58\ T_u \quad .$$

APPENDIX 6

TENDON PRESSURE UNDER RIBS

It is convenient for design to treat the crossed straight tendon ends in the anchor ribs as though they were a single continuous curved tendon, when computing their effect on the concrete. This introduces negligible inaccuracy.

Refer to Figure 2 and consider a single tendon at diameter d_o as representative of the band.

The inward force per unit length of curved tendon is given by:

$$F_c = 2T/d_o \quad .$$

The inward force on the rib due to the anchored tendons is $2T \sin(\theta r/2)$. If we assume this to be distributed over the arc length $(d_o/2)\theta r$ (which is reasonable considering the rigidity of the rib), the inward force per unit length is given by:

$$F_r = [\ 2T \sin(\theta r/2)\ ] \ / \ [\ d_o/2)\theta r\ ]$$

$$= \frac{2T}{d_o} \ \frac{\sin\frac{\theta r}{2}}{\frac{\theta r}{2}} \quad .$$

$$\text{Thus} \quad \frac{F_r}{F_c} = \frac{\sin\frac{\theta r}{2}}{\frac{\theta r}{2}}$$

$= 1.000$ for $\theta r = 10°$

$= 0.995$ for $\theta r = 20°$

$= 0.99$ for $\theta r = 30°$

$= 0.98$ for $\theta r = 40°$.

These values of $\frac{F_r}{F_c}$ apply for $n_z = 1$. For $n_z \geq 2$ and $\theta r \leq 40°$, or $n_z = 1$ and $\theta r \leq 20°$, this effect can be dismissed as negligible, that is, less than $\frac{1}{2}$ per cent. Any possibility of producing an error greater than $\frac{1}{2}$ per cent. is removed if F_r/F_c is taken to be 0.995, and allowed for in design. This can be done by reducing the value of tension assumed in the equivalent continuous curved tendon.

APPENDIX 7

EFFECTIVE AVERAGE TENDON TENSION

Figure 2 shows the space arrangement of the tendons and anchor ribs. Figure 15 gives a developed view, showing the variation of tendon tension around the vessel. Each line represents the mean tension of a band of n_b tendons, all anchored at the same level on the same two rib faces. The tendons represented by Figure 15 form a vertical 'zone' if closed into a self-contained arrangement. Each zone will occupy a vertical height h of the cylinder. They are characterized by a parameter n_z which is the number of bands of tendons crossing any between-ribs cross-section within a zone.

Figure 15 shows quite clearly the repetitive pattern of the tendon tensions, the unit being the tensions found between a rib centre line, and the next between-ribs centre line. The effective average tension at any angle ϕ measured from the rib centre line, is given by:

$$T_{ea} = \frac{T_{\theta_o}}{n_z}\left[J + \exp\left(-\mu(2I\phi_m - \frac{\theta r}{2} - \phi)\right) + \exp\left(-\mu(2I\phi_m - \frac{\theta r}{2} + \phi)\right)\right],$$

where:

1. I is given all the integer values from 1 to $\frac{n_z}{2}$ (to the nearest smaller integer).
2. The last term is omitted if n_z is even, that is, there must be a total of n_z terms in the brackets.
3. $J = 0.99 \quad \text{if } 0 < \phi < \theta r/2$
4. $J = \exp\left(-\mu(\phi - \frac{\theta r}{2})\right) \quad \text{if } \frac{\theta r}{2} < \phi < \phi_m$

Evaluations of T_{ea} are shown by Figure 16 for $\theta_r = \phi_m/2$ and different values of r and n_z. (Note that $r = \pi/\phi_m$). It can be seen that $T_{ea(max)}$ occurs just beside the rib in all cases, and that with a slight error in some unlikely cases, $T_{ea(min)}$ occurs on the between-ribs centre line. Thus J can always be taken as $\exp\left[-\mu\left(\phi - \frac{\theta r}{2}\right)\right]$ and ϕ put equal to $\frac{\theta r}{2}$ and ϕ_m to find respectively, the maximum and minimum values of effective average tension.

APPENDIX 8

DESIGN USING HELICAL TENDON ARRANGEMENT

For the P.C.P.V. at Oldbury, vertical and circumferential tendons in the cylinder wall were replaced by a single system of helical tendons. This had the advantage of removing tendon anchors from the vessel walls and making them more accessible. It has the disadvantage of difficult tendon tube placement.

Elementary equations for the design of such a vessel are developed here, and further comparisons made.

Refer to Figure 11, and first consider tendon force under ultimate conditions. Let n_h be the total number of helical tendons arranged in n_L layers; let C be the anchor spacing, radially and circumferentially, and let ϵ be the helix angle.

Vertical and horizontal force balances give:

$$n_h T_u \sin\epsilon = \frac{\pi}{4} p_u d_i^2 \quad . \qquad \ldots\ldots(1)$$

$$\frac{n_L}{C \tan\epsilon} T_u \cos\epsilon = \tfrac{1}{2} p_u d_i \quad . \qquad \ldots\ldots(2)$$

It is also quickly seen that

$$n_h = n_L \pi d_o/C \qquad \ldots\ldots(3)$$

$$\tan\epsilon = 2\frac{(H + 2t)}{d_o \theta_w} \quad . \qquad \ldots\ldots(4)$$

Equations 1, 2, 3, reduce to:

$$\frac{d_i}{d_o} = 2\tan^2\epsilon \quad . \qquad \ldots\ldots(5)$$

This equation gives the helix angle for greatest economy in tendons, to resist the ultimate pressure.

Consider now the inward pressure of the tendons on the concrete. As already seen, $T_{\theta_o} = 0.62\ T_u$ when tensioning, and $T_{\theta_o} = 0.58\ T_u$ for test design conditions (refer Appendix 5). If we assume tensioning from both ends, T_{max} will occur near the ends where θ_w is small, so:

$$T_{max} = 0.62\ T_u \quad , \qquad \ldots\ldots(6)$$

Continued...

APPENDIX 8 (Continued)

and T_{min} will occur half way down the wall at $\theta_w/2$, so:

$$T_{min} = 0.58\ T_u\ \exp(-\mu\ \theta_w/2\ \cos\epsilon) \quad . \qquad .....(7)$$

It can be shown that the inward force per unit length of tendon is $2\ T\ (\cos^2\epsilon)/d_o$. It follows that the equivalent inward pressure is given by:

$$p_s = 2\ n_L\ T(\cos^2\epsilon)/d_o\ C\ \sin\epsilon \quad . \qquad .....(8)$$

To ensure sufficient concrete to withstand the tendon crushing, using Equations 6 and 8 with the Lamé equation (Equation 3.9 of the text):

$$f_c = \frac{2.48\ n_L\ T_u\ d_o\ \cos^2\epsilon}{C(d_o^2 - d_i^2)\ \sin\epsilon} \quad . \qquad .....(9)$$

To ensure that the concrete does not crack for the test design pressure, using Equations 7 and 8 with the Lamé equation:

$$f_t = \frac{\left(2.32\ n_L\ T_u\ d_o\ \exp\left[-(\mu\ \theta_w/2\ \cos\epsilon)\right]\ (\cos^2\epsilon)/(C\ \sin\epsilon)\right) - p_{td}(d_o^2 + d_i^2)}{d_o^2 - d_i^2} \qquad .....(10)$$

Eliminating T_u between (9) and (10) and using (3) to eliminate n_L, we obtain:

$$p_{td}\ \frac{d_o^2 + d_i^2}{d_o^2 - d_i^2} = 0.94\ f_c\ \exp\left[-(\mu\ \theta_w/2\ \cos\epsilon)\right] - f_t \quad .$$

Put $\alpha = d_i/d_o$ in (4), (5) and (11), eliminate θ_w, and put $\mu = 0.20$:

$$\frac{\tan^4\epsilon + 0.25}{\tan^4\epsilon - 0.25} + \frac{f_t}{p_{td}} = 0.94\ \frac{f_c}{p_{td}}\ \exp\left[-0.40\ (\sin\epsilon)\ (H+2t)/d_I\ \cos^2\epsilon\right] \qquad .....(11a)$$

$$1/\alpha = 2\ \tan^2\epsilon \quad . \qquad .....(5a)$$

Equation 11a determines the integrity of the vessel and must be satisfied. Equation 5a expresses the condition for the minimum number of tendons to resist ultimate pressure, but may be contravened if more tendons are used.

Continued...

APPENDIX 8 (Continued)

Consider Equation 11a. Put f_c = 2500 p.s.i., f_t = -200 p.s.i., p_{td} = 1330 p.s.i., and write A for $(H+2t)/d_I$ (that is, A ≡ Aspect ratio):

$$\frac{\tan^4\epsilon + 0.25}{\tan^4\epsilon - 0.25} - 0.15 = 1.77\ \exp\left[-0.40\ A\ \sin\epsilon/\cos^2\epsilon\right] \quad .$$

ϵ must be $> 35°$ and $< 55°$, or the L.H.S. of this equation becomes negative, while the R.H.S. remains always positive.

Figure 17 shows that A must be ≦ 0.28 and $\epsilon = 45°$ to withstand the pressure conditions specified without exceeding design stresses. However, higher values of A are possible if f_c is increased, or p_{td} decreased, for example, if p_{td} is reduced to 920 p.s.i., corresponding to p_w = 700 p.s.i., A may be taken as 1.

But Equation 5a requires that $\epsilon = 27°$ for economy of tendons (taking $\alpha = 2$ as a representative value). If ϵ is taken as 45°, this more than doubles the number of tendons required to satisfy Equation 2.

Summary

A helical arrangement of cylinder wall tendons can only be used for squat vessels, (diameter ≧ overall height) and low pressures (p_w ≦ 700 p.s.i.). It would not make economic use of the tendons, and placement of the tendon tubes and the concrete around them would be difficult. It has the advantage of grouping all cylinder wall anchors into accessible chambers at the top and bottom of the wall.

APPENDIX 9

PENETRATION LINER THICKNESS

Refer to Figure 12 and consider a cylindrical steel liner of thickness t_p and diameter d_p in concrete subject to a compressive stress σ_c. The internal pressure is zero: σ_s is the direct compressive stress induced in the liner on the XX centre-line.

What must be the dimensions of the liner if there is to be no concentration of stress in the concrete? This requires strain compatibility, so that bending stresses can be neglected for the moment. Balance of forces and compatibility of strains require:

$$\sigma_c \, d_p = 2 \, \sigma_s \, t_p .$$

$$d_p \frac{\sigma_c}{E_c} = d_p \frac{\sigma_s}{E_s} .$$

These give $\frac{d_p}{2t_p} = \frac{\sigma_s}{\sigma_c} = \frac{E_s}{E_c} \approx 6$ for good concrete,

whence $t_p = d_p/12$ for strain compatibility.

But will a liner of this thickness withstand the crushing force of the concrete without buckling? This must also be considered.

Refer to Figure 13 and consider the stability of unit length of a quarter of the liner. Assume that the concrete is stressed both horizontally and vertically. Stability is maintained by the direct forces F_v and F_h (no shear), and by moments M_x and M_y, at the axes. Force balance gives:

$$F_h = R \, \sigma_h \qquad \ldots\ldots(1)$$

$$F_v = R \, \sigma_v \qquad \ldots\ldots(2)$$

Taking moments about the y-axis section:

$$M_x - M_y = \frac{R^2}{2} (\sigma_v - \sigma_h) . \qquad \ldots\ldots(3)$$

The moment at θ is given by

$$M_\theta = M_x + \frac{R^2}{2} \sin^2 \theta \, (\sigma_h - \sigma_v) \qquad \ldots\ldots(4)$$

M_x is an indeterminate quantity, but can be evaluated by the principle of least work.

Continued...

Strain energy $$U = \int_0^{\pi/2} \frac{M_\theta^2 \, R \, d\theta}{2 \, E \, I}$$

and $$\frac{\partial U}{\partial M_x} = \frac{R}{EI} \int_0^{\pi/2} M_\theta \frac{\partial M_\theta}{\partial M_x} \, d\theta = 0 .$$

From Equation 4 $\frac{M_\theta}{M_x} = 1$ and therefore $\int_0^{\pi/2} M_\theta \, d\theta = 0$.

Then $$M_x = \frac{R^2}{4} (\sigma_v - \sigma_h)$$

$$M_y = \frac{R^2}{4} (\sigma_h - \sigma_v)$$

$$M_\theta = \frac{R^2}{4} (\sigma_v - \sigma_h) \cos 2\theta .$$

For the case where $\sigma_v = \sigma_h$ the moment is always zero and strain compatibility can be achieved, putting:

$$t_p = d_p/12 .$$

For the case where $\sigma_v = k\sigma_h$ and putting $R = d_p/2$

$$M_{max} = M_\theta \quad \text{for } \theta = 45^\circ$$

$$= d_p^2 (1-k) \, \sigma_h/16 .$$

The maximum bending stress in the steel is given by:

$$\sigma_B = 6M_{max}/t_p^2$$

$$= 3\sigma_h (1-k) \, d_p^2/8t_p^2 .$$

The maximum direct stress in the steel σ_d will occur on the vertical centre line ($\theta = 90^\circ$) and is given by:

$$\sigma_d = F_h/t_p$$

$$= d_p \, \sigma_h/2t_p .$$

Continued...

APPENDIX 9 (Continued)

For $\sigma_v < \sigma_h$ the direct stress at $\theta = 45°$ will be less than this, but because $\sigma_d << \sigma_b$ the maximum total stress in the steel may be taken as:

$$\sigma_s = \sigma_b + \sigma_d$$

$$= \frac{\sigma_h d_p}{2t_p} \left[\frac{3d_p}{4t_p} (1-k) + 1 \right] .$$

Now the compressive stresses in the concrete σ_h and σ_v for no pressure in the vessel are given by the following formulae:

$$\sigma_h = 0.62 \epsilon \beta p_w \left(\frac{\alpha}{\alpha^2-1}\right) \left(\frac{d_i^2 + d^2}{d^2}\right)$$

$$\sigma_v = 0.62 \beta p_w/(\alpha^2-1) .$$

Then $$k = \sigma_v/\sigma_h = \frac{d^2}{d^2 + d_i^2} \Big/ \epsilon \alpha .$$

Figure 18 shows the penetration liner thickness ratio (t_p/d_p) required to resist deformation if mild steel is used with a yield stress of 42,000 p.s.i. The variation of this thickness, as well as the variation of concrete stress through the wall are shown for two different wall thickness ratios ($\alpha=d_o/d_i$). A thickness greater than $d_p/12$ must be used, and this will produce some stress concentration in the adjacent concrete.

For feasibility design it seems reasonable to assume all penetrations to have a thickness $d_p/10$. This is so because the liners are stiffened by anchor ribs and cooling pipes, which should make them adequately strong, and the stress thrown on to the concrete by this extra thickness can be handled by suitable reinforcement.

If more vertical tendons are used to control cracking between wall and end slabs, then the thickness of penetration liners could be reduced, that is, σ_v becomes more nearly equal to σ_h. In the end slabs themselves, thinner liners could certainly be used, but, again for simplicity, $t_p = d_p/10$ can be assumed for feasibility design.

APPENDIX 10

PENETRATIONS - TENSILE LOADING

The horizontal circumferential stress in the cylinder wall concrete σ_h at any diameter d for limiting internal pressure p_{td} is given by the Lamé equation:

$$\sigma_h = \frac{p_{s(td)} d_o^2 - p_{td} d_i^2 - (p_{td} - p_{s(td)}) \left(\frac{d_o d_i}{d}\right)^2}{d_o^2 - d_i^2} .$$

Making the design assumptions of this report, this reduces to:

$$\sigma_h = \left[0.58 \epsilon \beta \alpha (d^2+d_i^2) - \gamma (d^2+\alpha^2 d_i^2)\right] p_w/d^2 (\alpha^2-1) . \quad .....(1)$$

The vertical stress in the cylinder wall concrete σ_v assumed uniform between d_i and d_o for limiting internal pressure p_{td} is given by:

$$\sigma_v = \frac{4 n_v T_{v\,(td)} - \pi d_i^2 p_{td}}{\pi d_i^2 (\alpha^2-1)} .$$

This similarly reduces to:

$$\sigma_v = \left(\frac{0.58\beta - \gamma}{\alpha^2-1}\right) p_w . \quad .....(2)$$

Refer now to Figure 13 and consider the effect of pressure p_{td} inside a lined penetration. Neglecting bending moments, force balances give:

$$\sigma_h - p_{td} = \frac{2t_p}{d_p} f_h$$

$$\sigma_v - p_{td} = \frac{2t_p}{d_p} f_v ,$$

where f_h and f_v are circumferential stresses in the liner at the vertical and horizontal centre-lines respectively. Substituting for σ_h and σ_v,

$$f_h/p_w = \frac{d_p}{2t_p} (0.58 \epsilon \beta - \alpha\gamma) \left(\frac{d^2+d_i^2}{d^2}\right) \left(\frac{\alpha}{\alpha^2-1}\right)$$

$$f_v/p_w = \frac{d_p}{2t_p} \left[\frac{0.58\beta - \gamma\alpha^2}{\alpha^2-1}\right] .$$

Continued...

APPENDIX 10 (Continued)

Taking $\beta = 2.75$, $\gamma = 1.33$, $\epsilon = 0.80$, $d_p = 10t_p$,

$$f_h/p_w = (6.37-6.65\alpha)\left(\frac{\alpha}{\alpha^2-1}\right)\left(\frac{d^2+d_i^2}{d^2}\right)$$

$$f_v/p_w = (8.00-6.65\alpha^2)\left(\frac{1}{\alpha^2-1}\right) .$$

Taking the maximum value of $\frac{d^2+d_i^2}{d^2}$; $\left(\text{that is, } \frac{d^2+d_i^2}{d^2}\ \max = 2, \text{ when } d=d_i\right)$

and putting $\alpha = \left(\frac{2540 + \gamma p_w}{2540 - \gamma p_w}\right)^{\frac{1}{2}}$, the values of f_h and f_v for the range of vessel pressure of interest are shown by Figure 19. The tensile stress in the liner increases with increasing working pressure, but only to quite safe values. (Note that the assumption of ϵ constant at 0.8 causes an overestimation of f_h for higher pressures by about 20 per cent.

Now consider the case of pressure in an unlined penetration. This is the situation where the contained fluid has escaped through a tear in the vessel liner, and is pressurising a crack in the concrete behind the liner. The horizontal and vertical stresses in the concrete (σ_h and σ_v) are shown in Figure 20 (across the wall of the vessel for test pressure in the vessel and also for working pressure in the vessel). If this occurred under test pressure conditions, a vertical crack would form and propagate radially outwards. For values of α less than 1.5, this vertical crack would extend right to the outside, but for larger values of α, it would change to a horizontal crack part way through and then continue to the outside. Under working pressure conditions however, for α less than 1.5 (that is, $p_w <$ 740 p.s.i.g.) the crack would not propagate, but for thicker vessels (that is, $\alpha > 1.5$, $p_w >$ 740 p.s.i.g.) it would propagate right through, horizontally. This assumes that crack propagation depends on the establishment of a tensile stress in the concrete $\geq$ 600 p.s.i., and takes no account of stress concentration at the edge of a crack, or reinforcement, or thermal or other secondary stress effects.

To sum up, internal pressure does not overstress the lining of penetrations but pressure applied to an unlined penetration in a high pressure vessel due to a lining failure could drive a crack right through the wall.

APPENDIX 11

DERIVATION OF COST EQUATIONS

Cost of Concrete

Let the cost of concrete in position, be S_c (\$ per yd^3). Let the cost of formwork be S_f (\$ per 100 ft^2) of external surface, taken with a fixed cost of \$ S_{ff} for special forms. It is assumed that the cylinder wall would be poured by lifts, and that all internal forming is provided by the vessel lining.

The cost of concrete in dollars, is then:

$$C_c = \frac{Sc}{27}\left[\frac{\pi}{4}(D_o^2-d_i^2)\,H + r\,(H+6)\,(D_o-X)\,X\sin^2(\theta_r/2) + 2t_s\,\frac{\pi}{4}D_o^2\right]$$

$$+ \frac{S_f}{100}\left[\frac{\pi}{2}D_o^2 + \pi D_o\,(H+2t_s) + r(H+6)\left\{(D_o-2X)\sin\frac{\theta_r}{2} + 2X - \frac{D_o}{2}\,\theta_r\right\}\right]$$

$$+ S_{ff} .$$

Cost of Tendons

Let the cost of tendons (material only, delivered to site) plus tendon tubes in position, be S_{t+t} (\$ per foot).

Let the cost of anchors in position be S_a (\$ each).

Cylindrical Tendons

The number of cylindrical or hoop tendons, is given by:

$$n_h = r n_b\,(H + 6)\,12/h .$$

The length of each tendon, allowing 2 feet wastage at each anchor, is L_c + 4 feet.

The cost in dollars of cylindrical tendons and anchors, is given by:

$$C_{ct} = n_h(L_c + 4)\,S_{t+t} + 2\,n_h\,S_a .$$

Vertical Tendons

Cost in dollars of vertical tendons and anchors allowing 2 feet wastage at each anchor, is given by:

$$C_{vt} = S_{t+t}\,n_v\,(H + 2t_s + 4) + 2\,S_a\,n_v .$$

Continued...

APPENDIX 11 (Continued)

End Slab Tendons

Cost in dollars of end slab tendons and anchors, allowing 2 feet wastage at each anchor, is given by:

$$C_{et} = 2\, n_e(1.75\, d_i\, S_{t+t} + 2\, S_a)$$

Threading and Prestressing

Let the cost of threading the tendons through the tubes be S_t ($ per tendon).

Let the cost of prestressing be S_p ($ per live anchor) that is, all rib anchors, but only half those on the ends are 'live'.

The cost of threading and prestressing in dollars, is then:

$$C_{t+p} = S_t\,(n_h + n_v + 2n_e) + S_p\,(2n_h + n_v + 2\,n_e) \quad .$$

Tendon Monitoring

Let the cost of monitoring the tendons for relaxation be S_{tm} ($ per tendon). This might be some form of load cell applied to say one tendon in three or four, or an indicator on each anchor to show movement due to gross relaxation. Alternatively, the tubes might have dried air circulated through them to prevent corrosion, and 'tendon monitoring' would mean 'humidity monitoring'. In this latter case relaxations would be tested for by periodic re-jacking of random tendons.

The cost of tendon monitoring, in dollars, is given by:

$$C_{tm} = S_{tm}\,(n_h + n_v + 2n_e) \quad .$$

Cost of Reinforcement

Let S_r be the cost of deformed bars at the site, ($ per lb) and S_{rp} the cost of placing the bars ($ per lb).

The total cost of reinforcing, in dollars, is given by:

$$C_r = 0.28\, V_{tr}\,(S_r + S_{rp}) \quad ,$$

where V_{tr} is the total volume of reinforcing bars, (in ^{3}) yet to be calculated.

Crack Control Reinforcement

Take crack control reinforcement as 0.25 per cent. of cross sectional area of wall in two directions. Volume of steel in the walls is given by:

$$V_{sw} = \frac{2 \times 0.0025}{4}\,\pi\left(D_o^2 - d_i^2\right) H \quad ft^3 \quad .$$

Continued...

APPENDIX 11 (Continued)

For the end slabs, take a hypothetical extra wall height h_e, such that:

$$\pi\left(\frac{D_o + d_i}{2}\right) h_e = \frac{\pi}{4} D_o^2 \quad .$$

Then the total volume of crack control reinforcement steel, allowing for overlap, is given by:

$$V_{ccs} = \frac{0.005}{4}\,\pi\left(D_o^2 - d_i^2\right)\left(H + \frac{D_o^2}{D_o + d_i}\right)\frac{23}{20} \quad ft^3 \quad .$$

Rib Binding Steel

Steel running around the surface of the ribs to control cracks and to bind the ribs to the wall is additional to anchor reinforcement.

Assume $\frac{7}{8}$ inch $\emptyset$ bars spaced at 9 inches in both directions; (this is a hypothetical uniform spacing which would be greatly varied in practice to avoid anchors). Then steel volume per unit area of rib face:

$$= \frac{2 \times 9 \times \frac{\pi}{4} \times (\frac{7}{8})^2}{9 \times 9 \times 12} = 0.011 \quad ft^3/ft^2 \quad .$$

If the horizontal bars are assumed to project 3 feet into the wall, the volume of rib binding steel is given by:

$$V_{rbs} = 0.011\, r\,(H+6)\,(a+2X+3) \quad ft^3$$
$$= 0.011\, r\,(H+6)\left((D_o - 2X)\sin\frac{\theta_r}{2} + 2X + 3\right) \quad ft^3 \quad .$$

Anchor Reinforcement

For calculating anchor reinforcement, Cable Covers Ltd. anchors are assumed and the method set out in their pamphlet Tension (No 10), is used.

A cube of concrete of dimensions 2a is associated with each anchor, where 2a is given by:

$$2a = \sqrt{(\text{Anchor face area})/(\text{Number of anchors})} \quad .$$

The area of steel in each cube is found from a curve (approximated by an analytic expression for computer use) as a function of 2a'/2a, where 2a' is the dimension of the anchor plate (assumed to be square). For the 12/0.6 inch tendons used, 2a'=11 inches.

Continued...

APPENDIX 11 (Continued)

The volume of steel per anchor is taken to be 2a x function $(\frac{11}{2a})$ in ^{3}.

The volume of rib anchor steel is given by:

$$V_{ras} = \frac{2\,n_h}{n_b}\sqrt{12hX}\ \text{function}\left(11 \Big/ \sqrt{\frac{12hX}{n_b}}\right) .$$

The volume of vertical tendon anchor steel is given by:

$$V_{ras} = 2n_v \sqrt{144\pi\left((d_o-X)^2-(d_i+6)^2\right) \Big/ 4n_v}$$

$$\text{function}\left[11 \Big/ \sqrt{144\pi\left((d_o-X)^2-(d_i+6)^2\right) / 4n_v}\right]$$

The volume of end tendon anchor steel is given by:

$$V_{eas} = 4n_e \sqrt{S_h S_v}\ \text{function}\left(11 \Big/ \sqrt{S_h S_v}\right) .$$

Cost of Wall Liner

The cost of the $\frac{3}{4}$ in. thick M.S. liner, with stiffening/anchor ribs, was estimated in detail, allowing for cost of material and plate preparation (cutting and forming, with jig checking) in the workshop, transport to site, site fabrication and erection, and leak testing of welds. Shop labour rates were increased to allow for the non-repetitive nature of the job. Site welding costs were further increased because of the relative inefficiency of such work, and site handling and erection costs were yet further increased to allow for the large size of the 'vessel' and the extra scaffolding and staying required. With these allowances, the overall cost per ton was between $A900 and $A1,000, which compares reasonably with similar costs given by Kaiser Engineer (1962).

The most simple way of handling the liner cost, for the computer would be to take a unit cost S_L ($ per lb) and use the following expression for C_{wL}, the cost of the liner in dollars:

$$C_{wL} = S_L \times 0.28 \times 144\,(2\tfrac{\pi}{4} d_i^2 + \pi d_i H)\, t ,$$

where t is a thickness greater than $\frac{3}{4}$ in. to allow for the ribs. However, S_L can be little more than a guess unless a detailed cost is calculated for at least one case.

Continued...

APPENDIX 11 (Continued)

The expression used, derived from such a costing, is:

$$C_{wL} = 10\,d_i^2 + 72\,d_i H + 162\left[d_i + \sum_{J=1}^{J=\frac{d_i}{2}}\left\{\left(\frac{d_i}{2}\right)^2 - J^2\right\}^{\frac{1}{2}}\right] .$$

Cost of Penetration Liners

The length of the penetration is L_p and its diameter d_p. The liner is a welded M.S. tube of thickness $d_p/10$. Welded to this tube on the outer end is a forged extension of length d_p, with pressure flange. The forging is heavily anchored back into the concrete from another flange with ties $L_p/2$ long, of diameter $d_p/20$, spaced every 6 inches at diameter d_p.

Allowing for fabrication, radiographing of the weld between tube and forging, stress relieving, erection, and leak testing of the weld to the wall liner, the following expression for the cost of each penetration in dollars, was derived:

$$C_{pL} = 10^{-3}\left[4\,d_p^3 L_p + 172\,d_p^2 L_p + 420\,d_p^3 + 14{,}440\,d_p L_p + 15{,}280\,d_p\right]$$

The following table giving the number of each type of penetration, and the values of d_p and L_p, was derived for the reference design. They are related, more or less accurately in different cases, to given parameters of the design. A similar table would be required for any vessel so handled, because the penetration liners can contribute a very high proportion of the vessel cost.

Total penetration liner cost = $\sum C_{pL}$ for all penetrations.

TYPE	NUMBER	DIAMETER - d_p	LENGTH - L_p
Ball outlets	7	$8\,d_b + 4$	t_s
Ball inlets	9	$3.5\,d_b + 3$	t_s
Shut-down rods	13	$\frac{12 \times MW(e)}{200} + 4$	t_s
Shim rods	6	$\frac{6 \times MW(e)}{200} + 3$	t_s
Gas control valves	$\frac{6.9 \times 10^{-6}(\text{by-pass flow})}{\rho\ \text{gas}}$	12 inches	t_s

APPENDIX 11 (Continued)

TYPE	NUMBER	DIAMETER - d_p	LENGTH - L_p
Boiler tubes	7 x Banks	$\frac{18 \times MW(e) \times 6}{200 \times Banks}$	$\frac{D_o - d_i}{2}$
Circulators	$\frac{3.8 \times 10^{-4} (gas\ flow)}{(d_p - 6)^2 \rho\ gas}$	$42\ d_I/28$	$\frac{D_o - d_i}{2}$
Neutron detectors	12	8 inches	$\frac{D_o - d_i}{2}$
Total number	120 for ref. design		

Cost of Liner Insulation

Let S_{hi} and S_{vi} be the cost ($ per ft^2) of laminated S.S. insulation in position on horizontal and vertical wall surfaces respectively. Let S_{pi} be the cost ($ per ft^2) of similar insulation applied to the penetrations. Total insulation costs are then given in dollars by:

$$C_{wi} = \frac{\pi d_i}{2} \left[d_i S_{hi} + 2HS_{vi} \right]$$

$$C_{pi} = \frac{\pi}{12} S_{pi} \sum (d_p L_p) \text{ for all penetrations.}$$

Cost of Vessel Cooling Pipes

A detailed estimate of the cost of piping welded to the wall liner, and to the penetration liners, and also of the connecting pipes running out through the concrete, resulted in the following expression for the reference design and variations of it:

$$C_{vp} = 2\pi d_i \left[2H + \sqrt{t^2 + \left(\frac{D-d_i}{2}\right)^2} \right] + 4 \left[d_i + 4 \sum_{J=1}^{J=\frac{d_i}{2}} \sqrt{\left(\frac{d_i}{2}\right)^2 - J^2} \right]$$

$$\left[1 + \frac{1}{6d_i} \sqrt{t^2 + \left(\frac{D-d_i}{2}\right)^2} \right] + 2.5\ \Sigma\ (L_p d_p) \text{ for all penetrations.}$$

Continued...

APPENDIX 11 (Continued)

Cost of External Cooling Water Circuit

Cost of the external cooling water circuit is relatively small so its estimation was not detailed. Lengths of pipe, number of valves and fittings, and numbers of heat exchangers, tanks and pumps were given reasonable unit cost values, and totalled $A29,000. Installed cost was then taken as 3 x $A 29,000, or roughly $A 90,000. This cost was then assumed to vary with the two-thirds power of reactor output.

$$C_{CC} = 90{,}000 \left[\frac{MW(e)}{200} \right]^{2/3}$$

Conclusion

All the preceding costs were summed by a computer programme, enabling optimisation of the design. No allowance was made for temperature monitoring in the concrete. If this were considered to be necessary, it would have to be added to the cost.

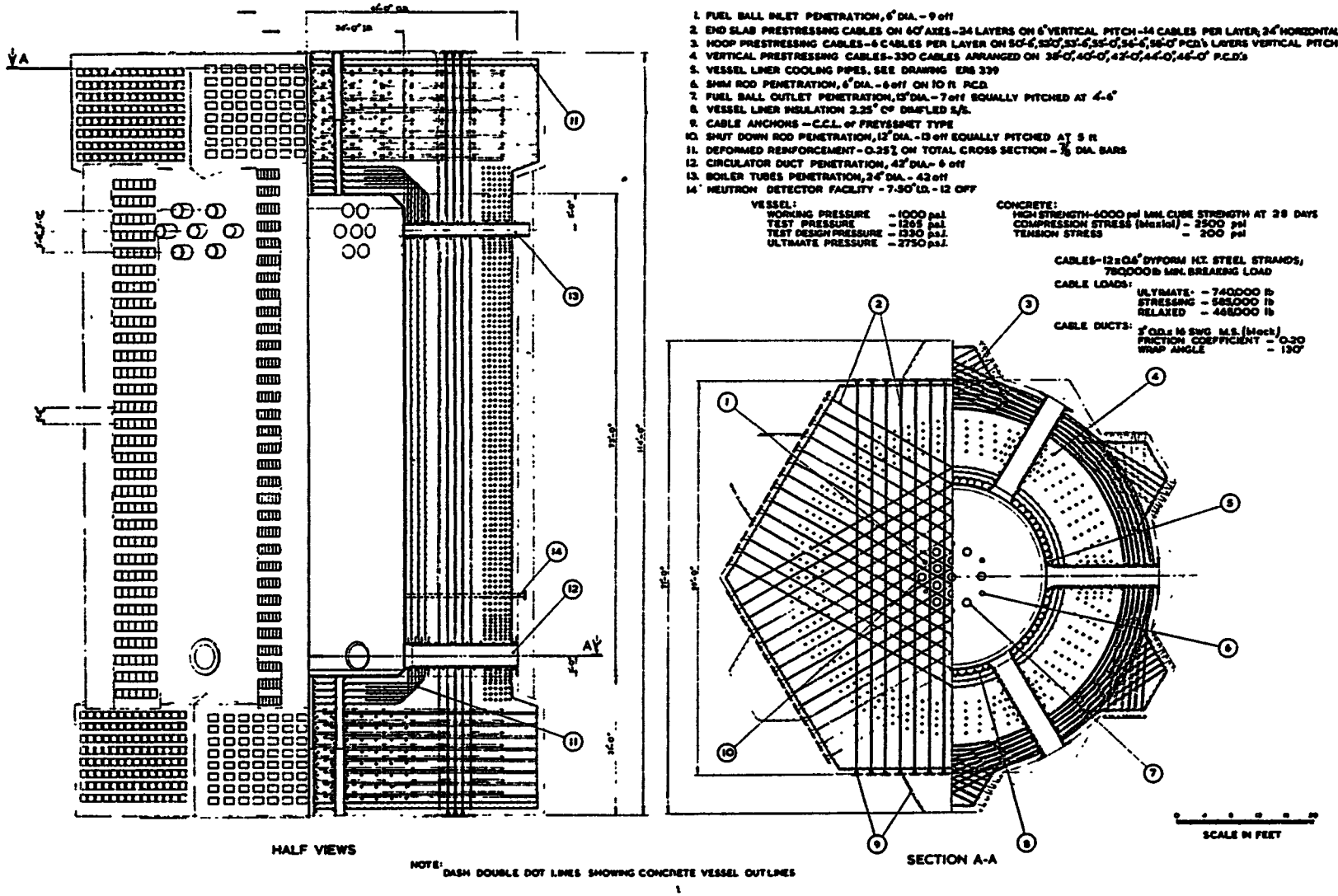

FIGURE 1. PRE-STRESSED PRESSURE VESSEL ARRANGEMENT FOR A 200 MWe PEBBLE BED REACTOR

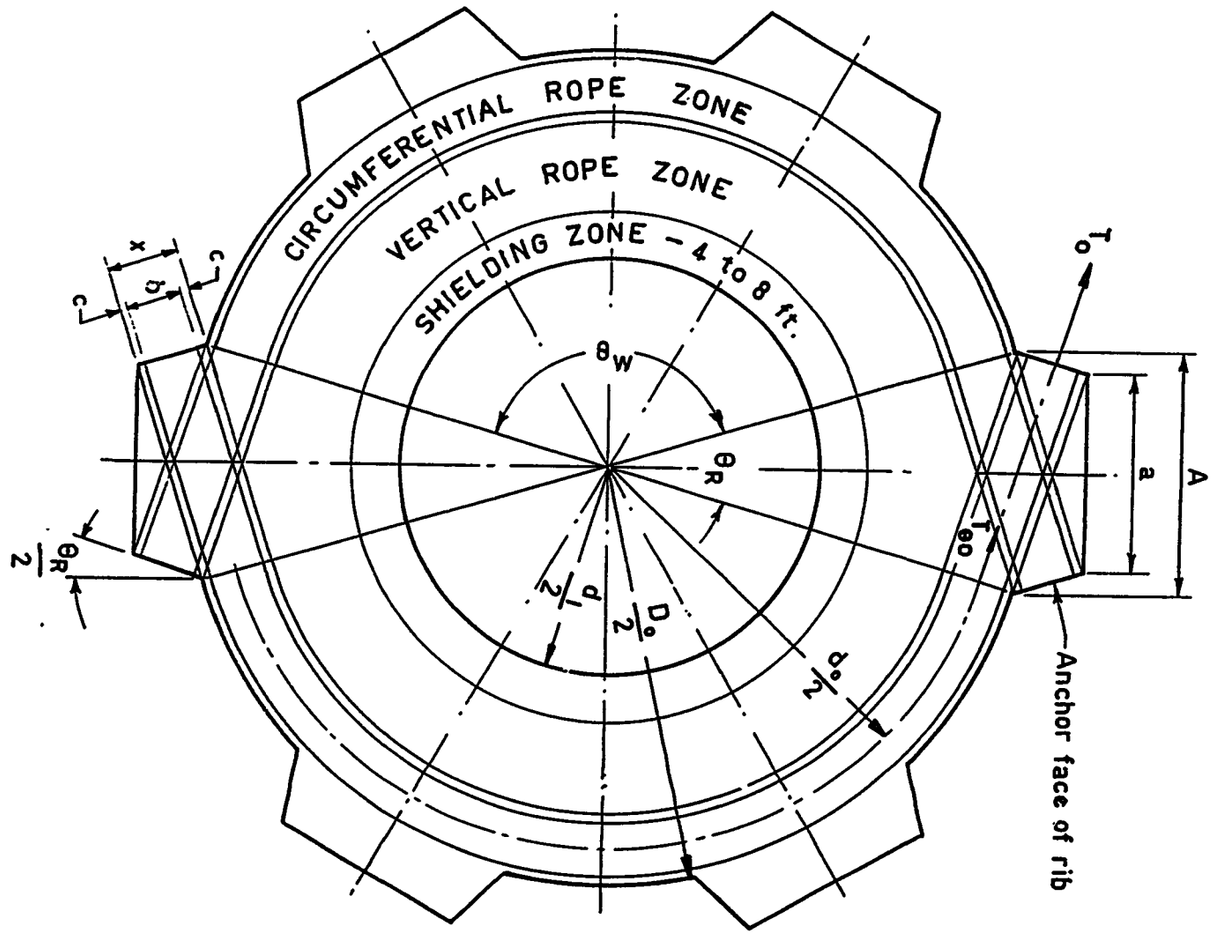

FIGURE 2. RIB AND TENDON ARRANGEMENT

P1043 (Drawn for r=6 and $(\theta_W+\theta_R) = 180^\circ$ but these can be varied)

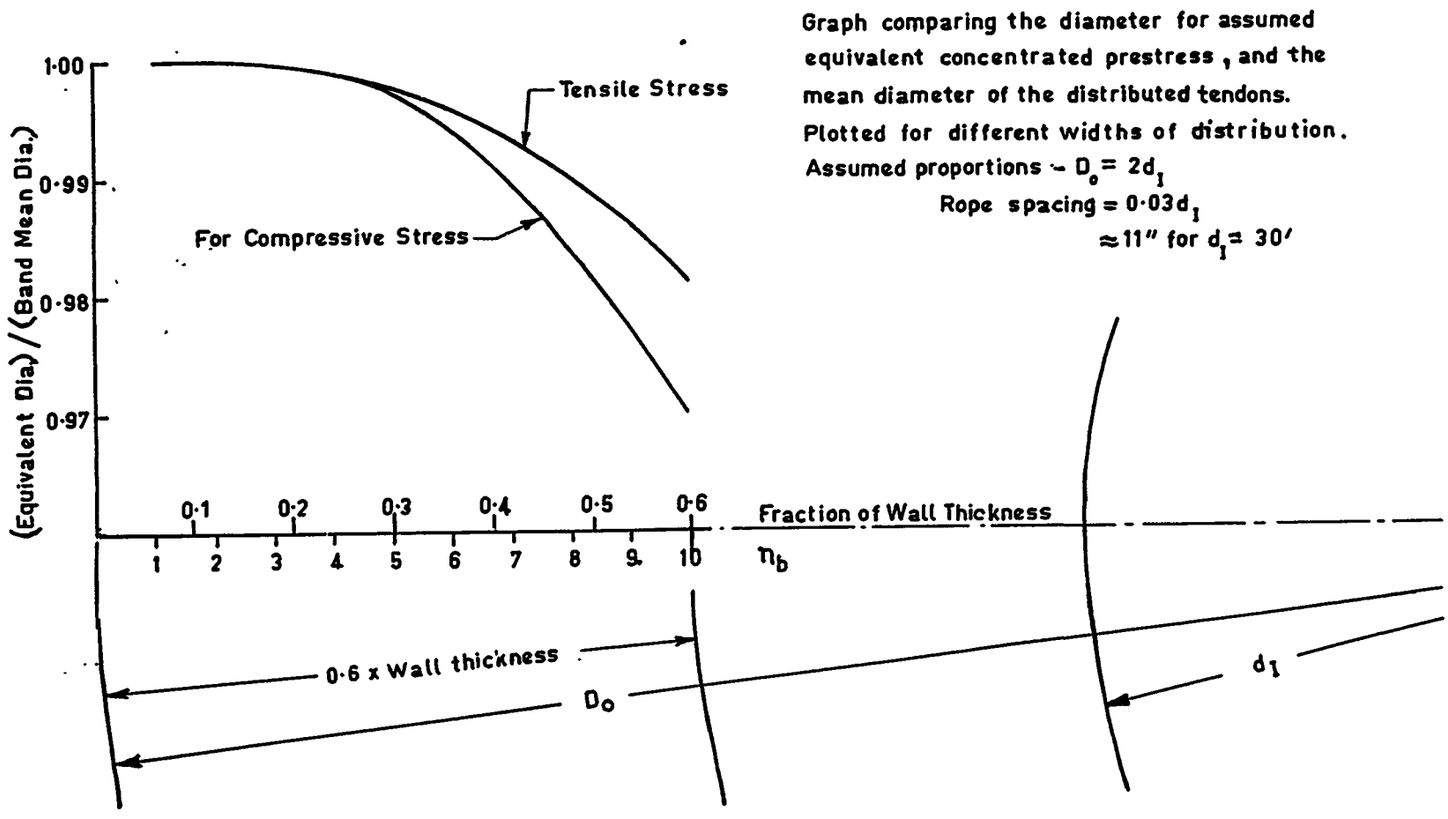

Graph comparing the diameter for assumed equivalent concentrated prestress, and the mean diameter of the distributed tendons. Plotted for different widths of distribution.

Assumed proportions – $D_o = 2d_1$

Rope spacing = $0{\cdot}03d_1$

$\approx 11''$ for $d_1 = 30'$

FIGURE 3. EFFECT OF DISTRIBUTED PRE-STRESS

P1043

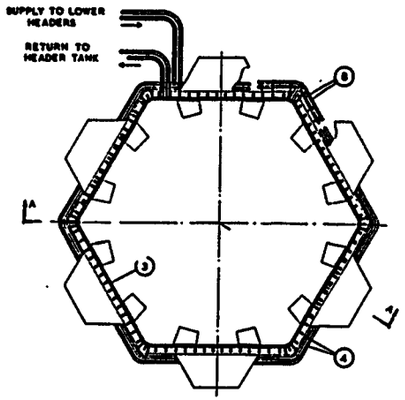

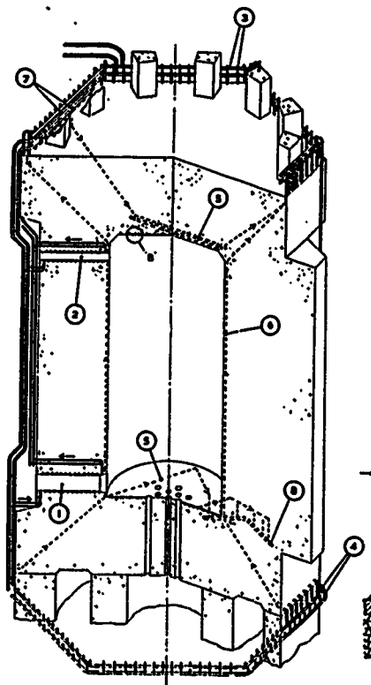

SECT. AA.

DIAGRAMMATICAL ARRANGEMENT OF VESSEL COOLING TUBES

1. CIRCULATOR PENETRATION
2. STEAM PIPE PENETRATION
3. UPPER HEADERS - OUTLET
4. LOWER HEADERS - INLET
5. VESSEL END SLAB COOLING TUBES
6. VESSEL VERTICAL WALL COOLING TUBES
7. INLET HEADER - TOP SLAB COOLING
8. OUTLET HEADER - BOTTOM SLAB COOLING

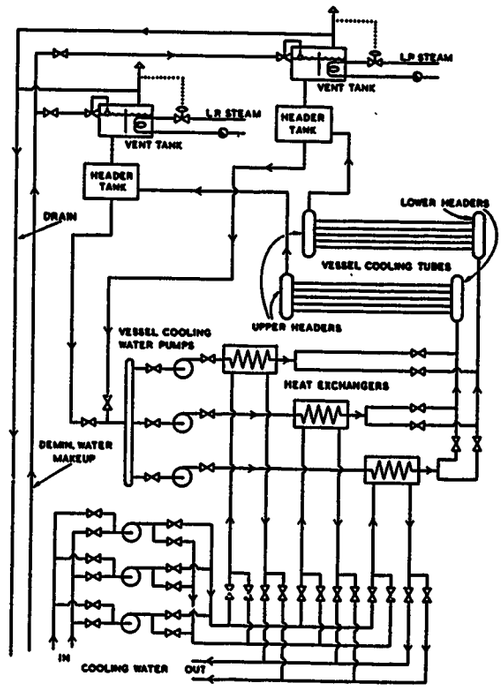

VESSEL COOLING WATER SYSTEM — SCHEMATIC

LEGEND
- LEVEL CONTROL VALVE
- BOILING CONTROL VALVE
- STEAM TRAP

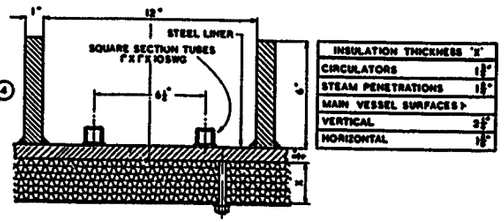

DETAIL 'B'

SHOWING ARRANGEMENT OF STAINLESS STEEL FOIL INSULATION, MILD STEEL VESSEL LINER AND LINER ANCHOR RIBS, AND COOLING WATER PIPES

NOTE:
PRESSURE VESSEL INTEGRITY IS DEPENDENT ON THE CONCRETE COOLING. BECAUSE OF THIS, THE COOLING SYSTEM IS DUPLICATED AT EVERY POINT. ONE SYSTEM, OPERATING ON ITS OWN, IS SUFFICIENT TO HOLD THE CONCRETE TEMPERATURE TO A SAFE VALUE. (60°C OR PERHAPS 70°C. NORMALLY OPERATES AT ABOUT 50°C)
PENETRATION LINERS COOLED AS (1) AND (2) BUT NOT SHOWN, ARE CONTROL RODS, BALL FEED MECHANISMS, SHIM RODS, CO_2 VENTS AND SINGLERS.

FIGURE 4. PRE-STRESSED PRESSURE VESSEL INSULATION AND COOLING FOR A 200 MWe PEBBLE BED REACTOR

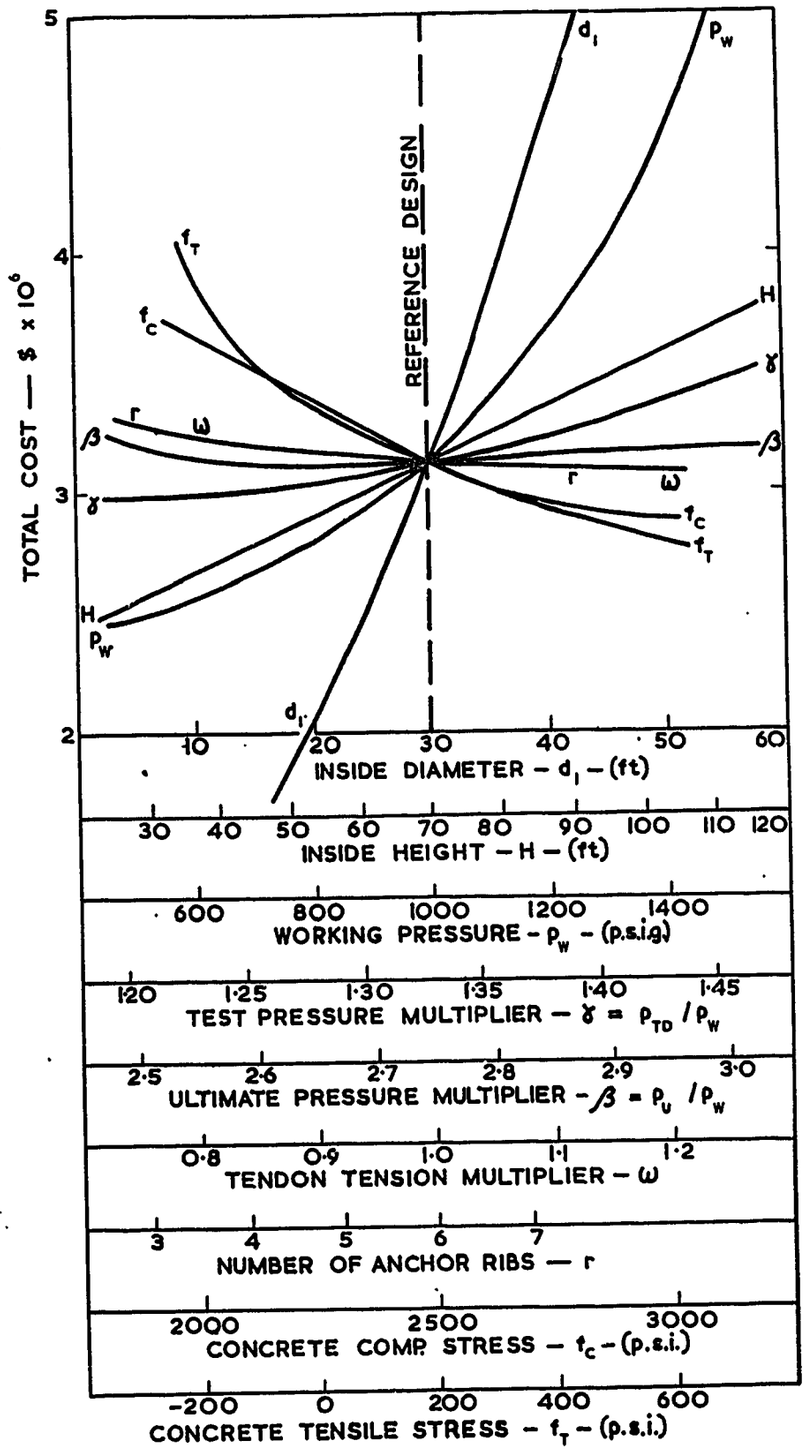

FIGURE 5. COST VARIATIONS ABOUT THE REFERENCE DESIGN (Parameters Varied One at a Time)

P1041

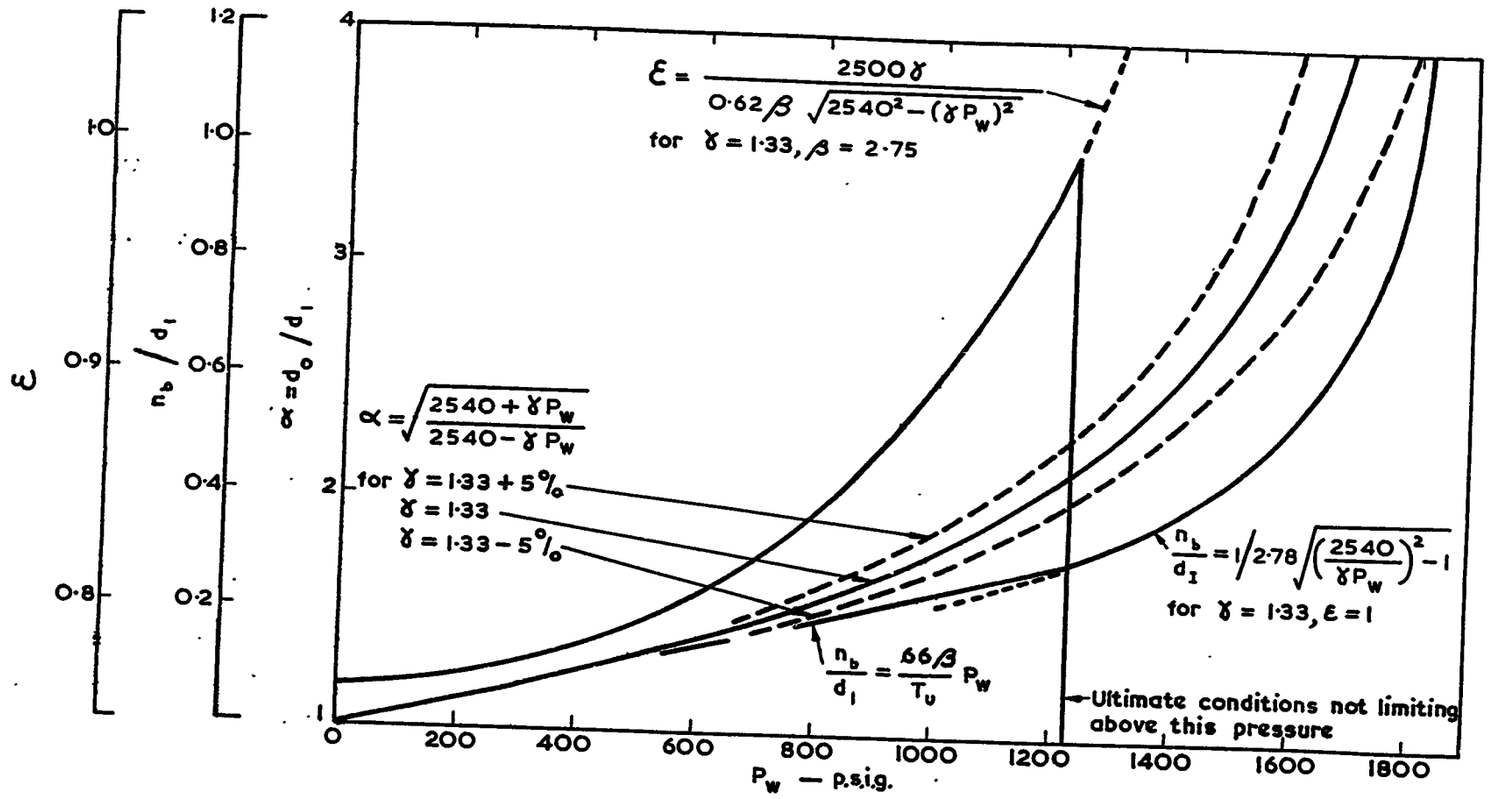

FIGURE 6. SOLUTIONS OF ANALYTIC DESIGN EQUATIONS

P1043

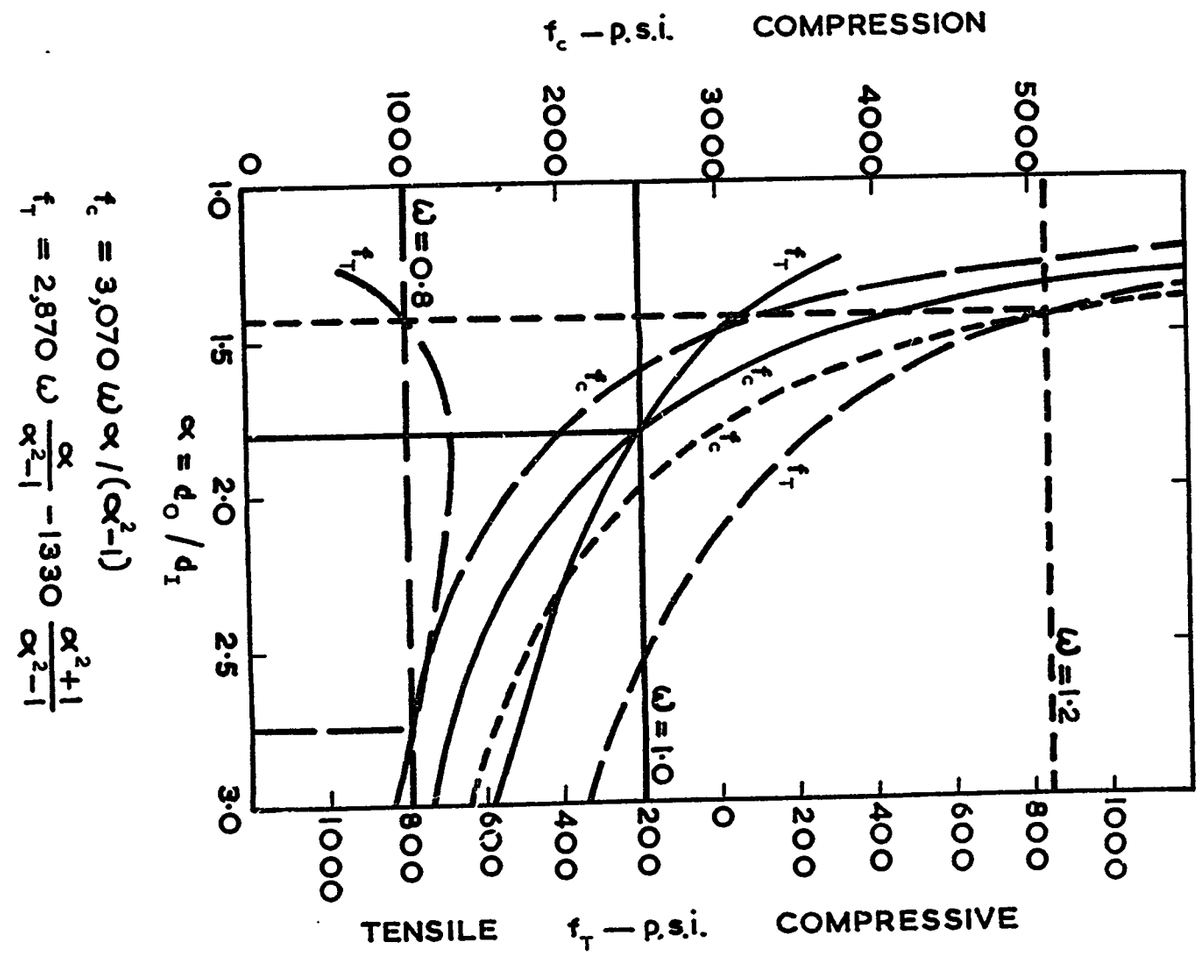

$$f_c = 3{,}070\,\omega\,\alpha/(\alpha^2-1)$$

$$f_T = 2{,}870\,\omega\,\frac{\alpha}{\alpha^2-1} - 1330\,\frac{\alpha^2+1}{\alpha^2-1}$$

FIGURE 7. SOLUTIONS FOR CYLINDER WALL THICKNESS

P1043

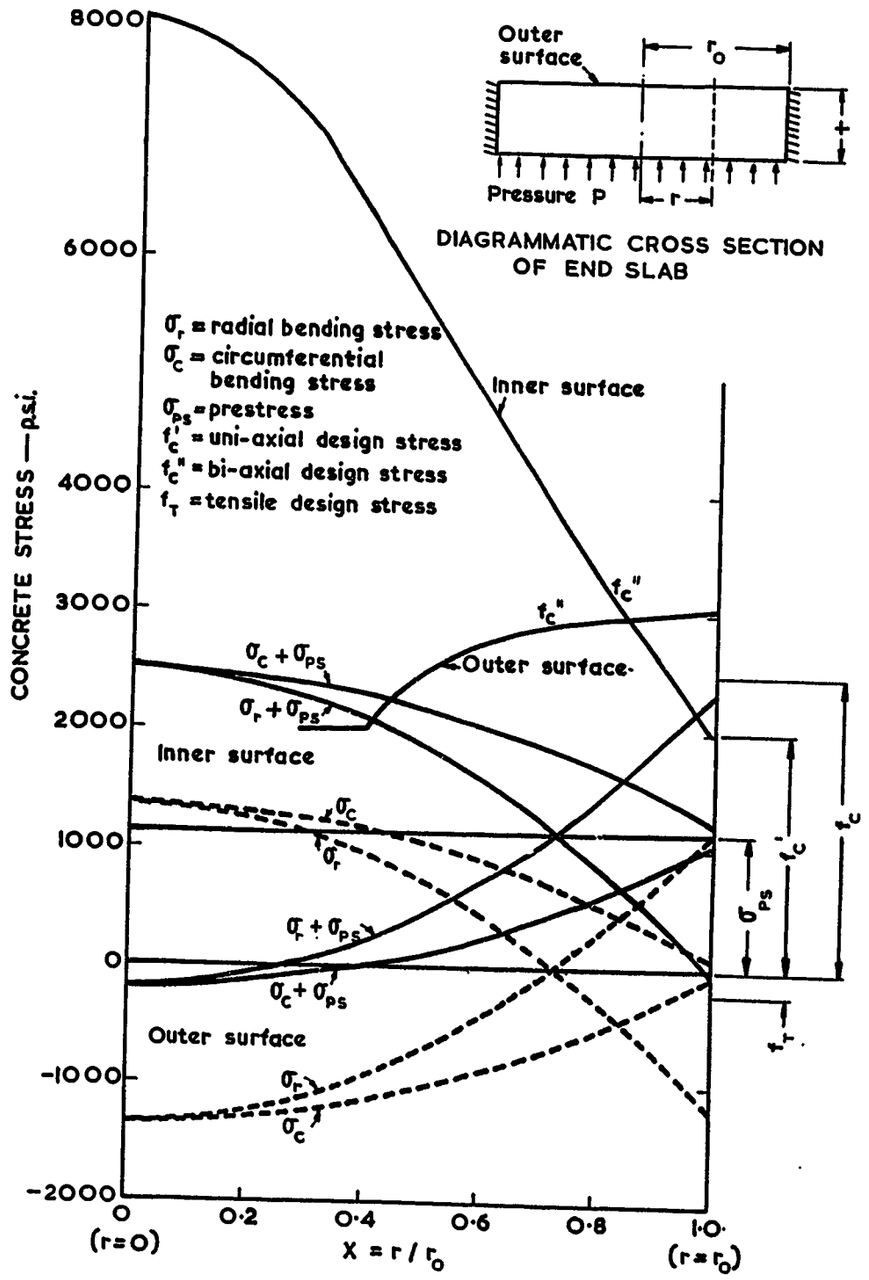

FIGURE 8. STRESSES IN END SLABS

P1043

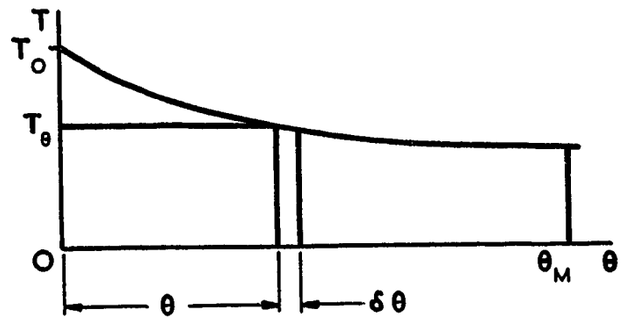

FIGURE 9. TENDON TENSION-EFFECT OF DUCT FRICTION

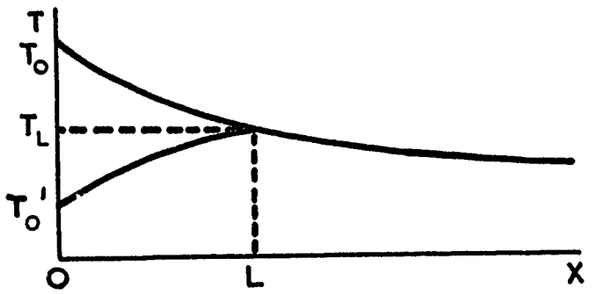

FIGURE 10. TENDON TENSION-EFFECT OF ANCHOR SET

P1043

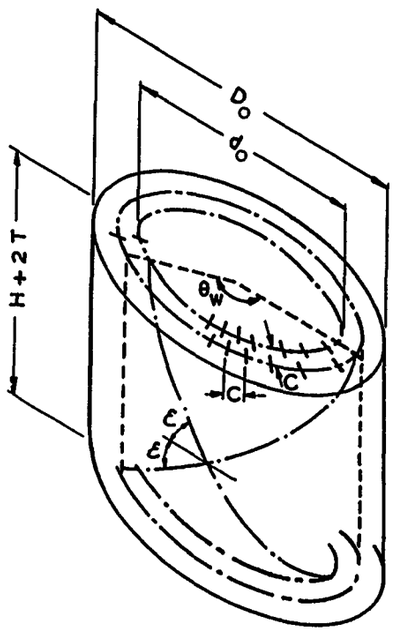

FIGURE 11. ARRANGEMENT PARAMETERS FOR HELICAL TENDONS

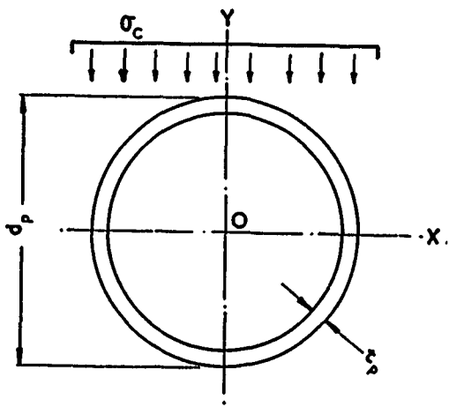

FIGURE 12. PENETRATION LINER UNI-DIRECTIONAL CONCRETE STRESS

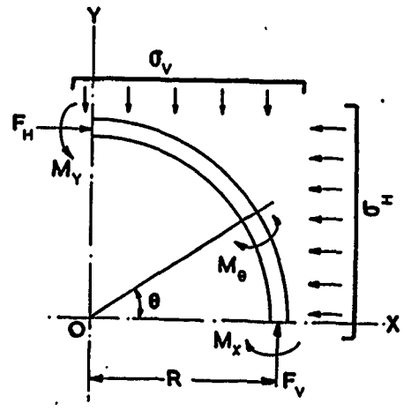

FIGURE 13. PENETRATION LINER BI-DIRECTIONAL CONCRETE STRESS

P1043

T_0 = Jacking tension. T_0^1 = Relaxed anchor tension after set δ

T_L = Tension at length L from anchor, where T_L is maximum tension unaffected by the relaxation due to δ.

$$\delta = \frac{T_0}{KAE}(1-e^{-KL})e^{-KL} \qquad T_L = T_0 e^{-KL} \qquad T_0^1 = T_0 e^{-2KL}$$

For 0·06 Dyform strand $T_0 = 0{\cdot}80 \times 65.000$ lb, $A = 0{\cdot}253$ in^2, $E = 28 \times 10^6$ p.s.i. $\Big\}$ $\frac{T_0}{AE} \simeq 7{\cdot}34 \times 10^{-3}$

For 'straight' tendon, $K = 10^{-3}$ ft^{-1} $\longrightarrow$ $T_0 / KAE = 7{\cdot}34$ ft.

For values of interest (i.e. practical anchor sets, and 'K' values.): $T_L/T_0 \simeq 1 - KL$; $T_0^1/T_0 \simeq (1-KL)^2$; $\frac{KAE}{T_0} \times \delta \simeq KL(1-KL)$

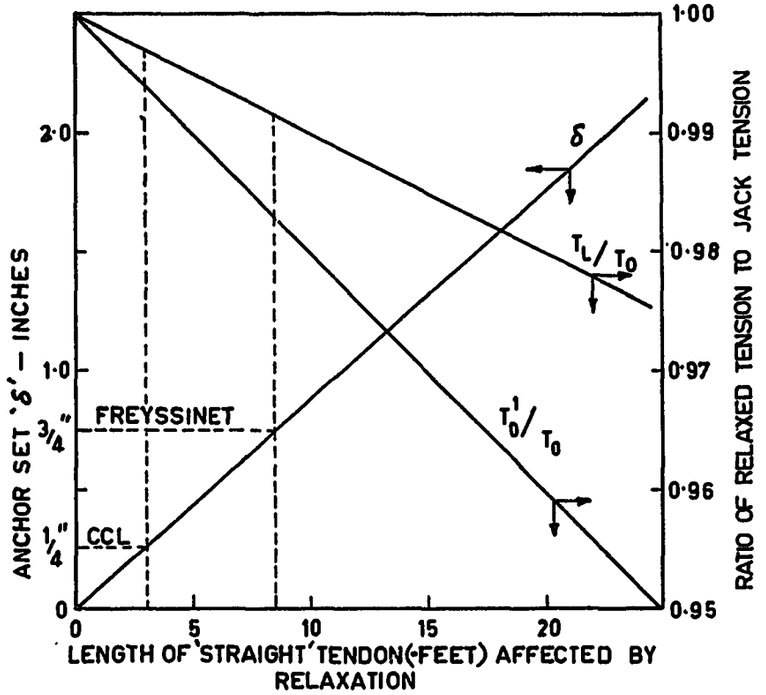

FIGURE 14. RELAXATION OF TENDON TENSION DUE TO LIVE ANCHOR SET

P1043

Tendon tension is plotted vertically on a development at diameter d_o. There are two basic arrangements, one for n_z even, and one for n_z odd. In both cases, the "pattern" is repetitive from rib ℄ to between-ribs ℄. This angle has been called ϕ_M. The sum of tendon tensions at any angle ϕ, measured from rib ℄, has been calculated and plotted for values of ϕ from 0 to ϕ_M. These plots represent all tensions anywhere around the vessel. Note that $\phi_M = \frac{\pi}{r}$.

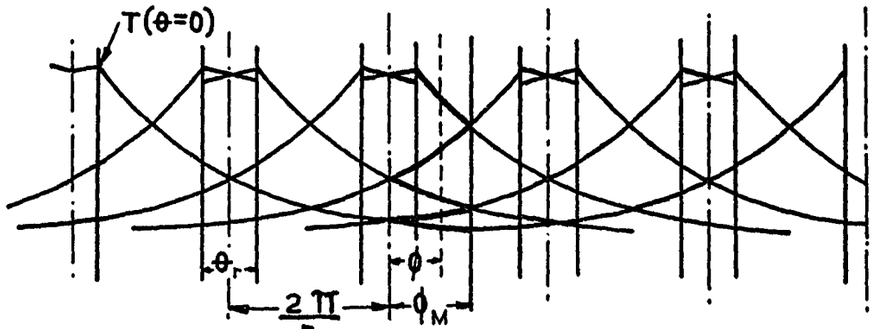

n_z = an odd number (= 5 as drawn)
r = odd or even number

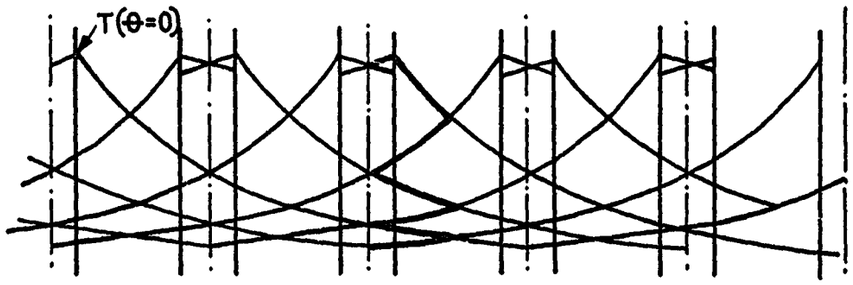

n_z = an even number (= 6 as drawn)
r = an odd or even number

FIGURE 15. AVERAGE EFFECTIVE TENDON TENSION

P1043

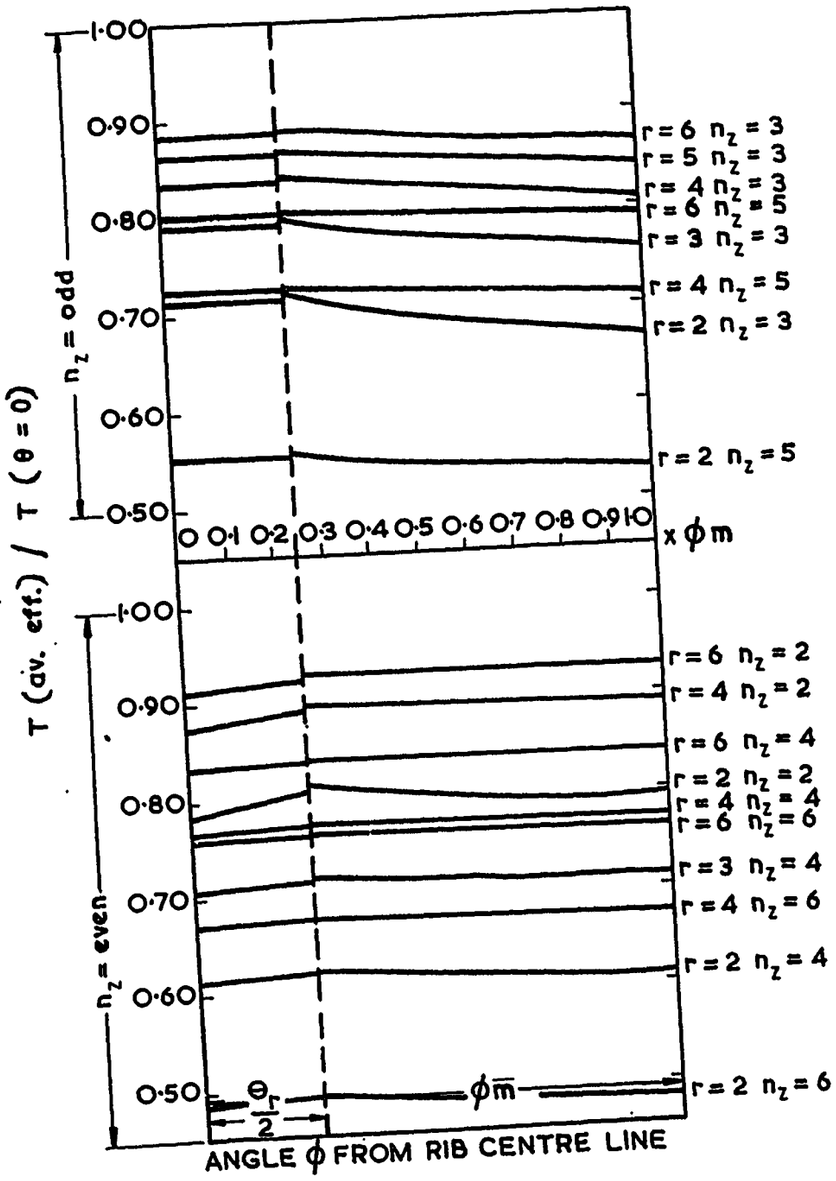

FIGURE 16. AVERAGE EFFECTIVE TENDON TENSION FOR $\theta_r = \phi_m/2$

P1043

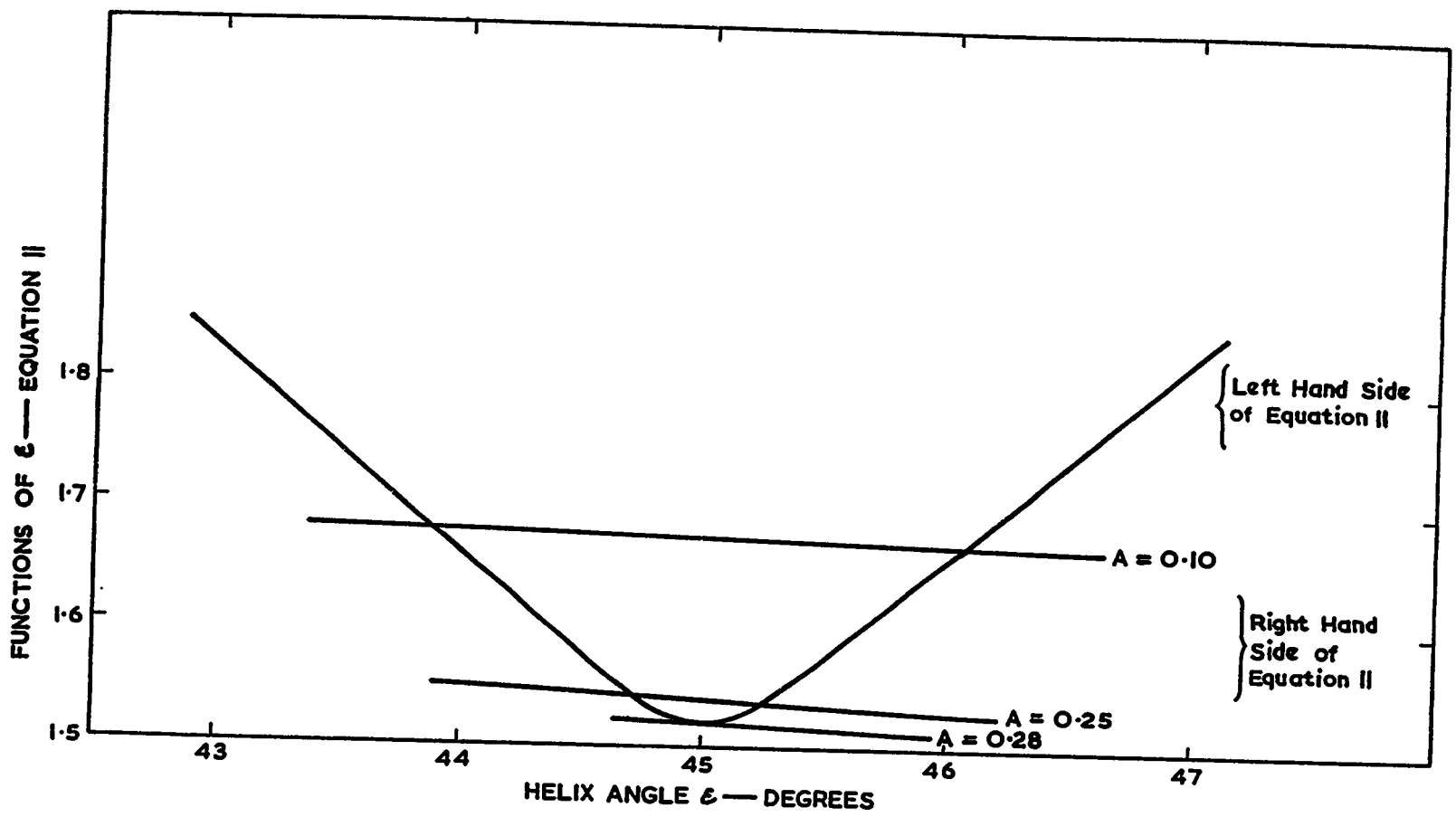

FIGURE 17. ASPECT RATIO LIMITS FOR HELICAL TENDON ARRANGEMENT
P1043 **(Solutions of Equation 11 from Appendix 8)**

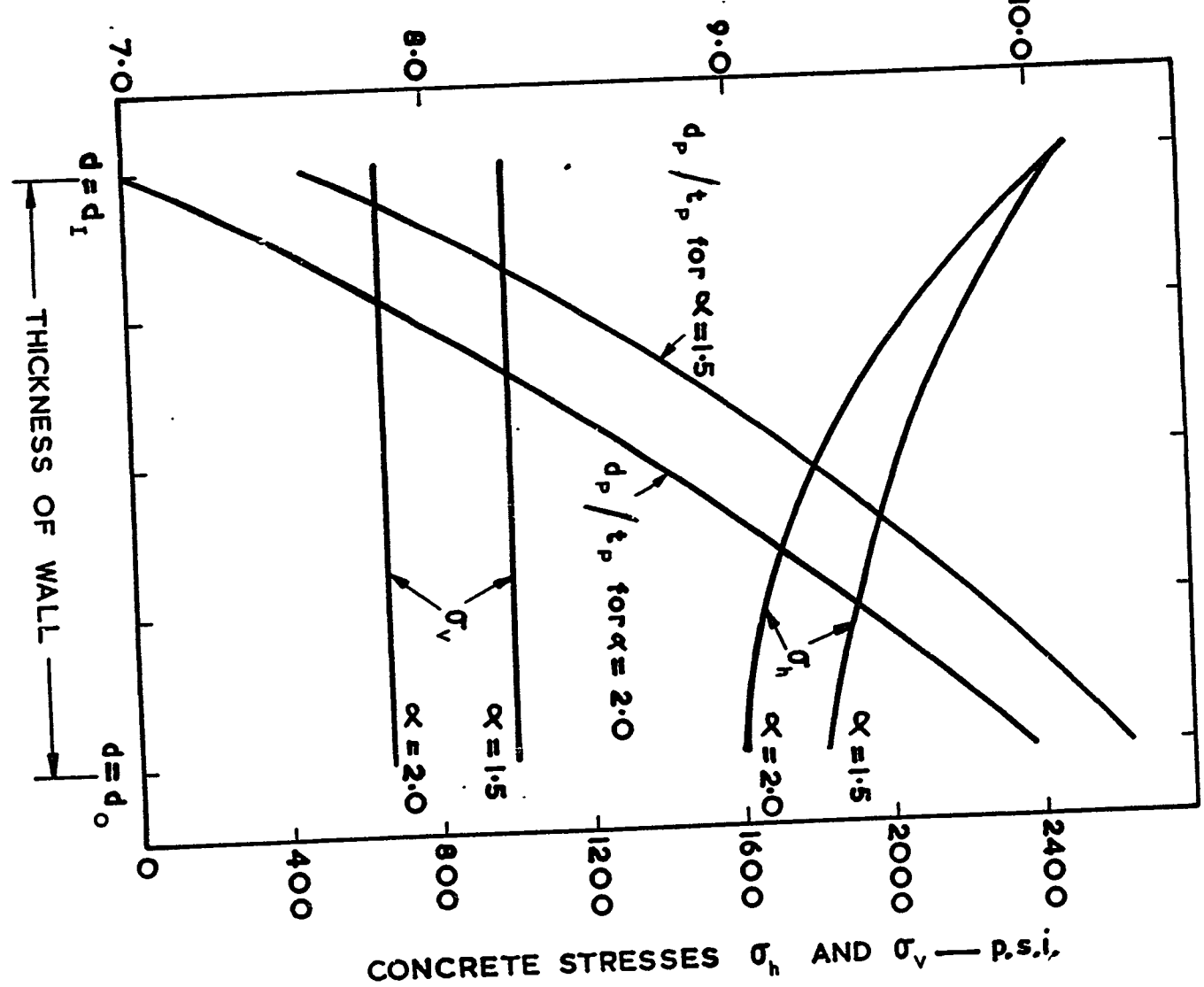

FIGURE 18. PENETRATION LINER THICKNESS TO RESIST BUCKLING
P1043

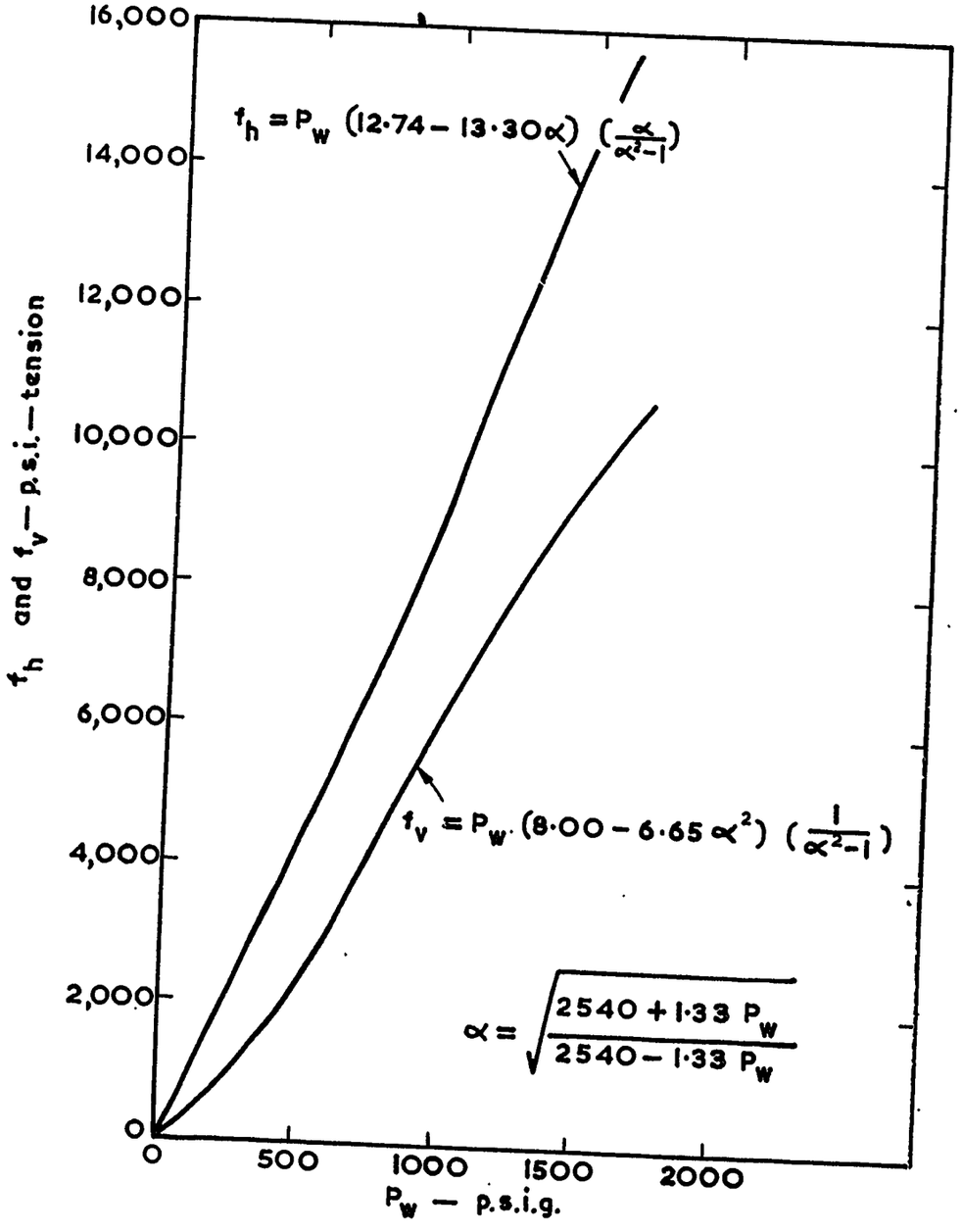

FIGURE 19. CIRCUMFERENTIAL TENSILE STRESSES IN PENETRATION LINERS

P1043

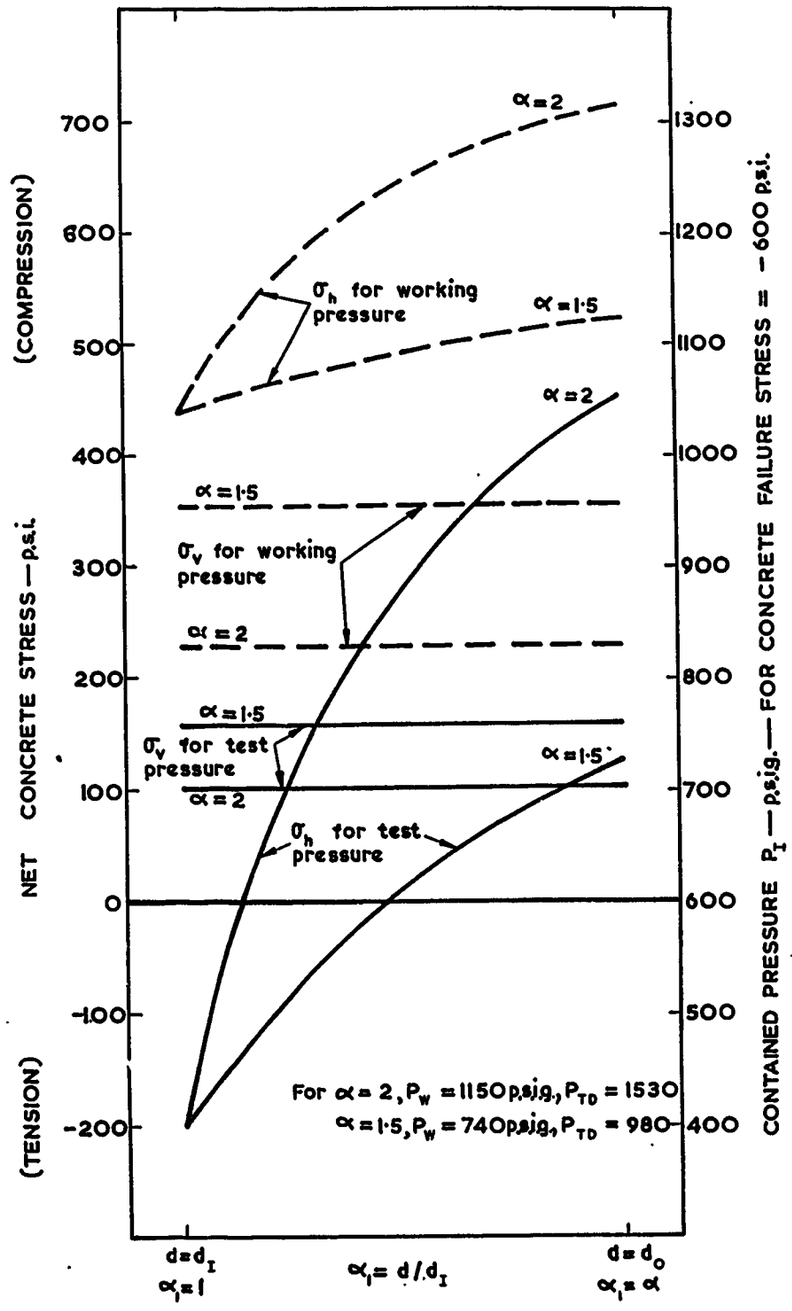

FIGURE 20. CONCRETE STRESS IN CYLINDER WALL FOR TEST PRESSURE AND FOR WORKING PRESSURE

P1043